TALLINN UNIVERSITY OF TECHNOLOGY
School of Information Technologies

Ritu Rani, 184605IVEM

SOFTWARE DEFINED RADIO BASED REALIZATION OF DIGITAL SELF-INTERFERENCE CANCELLATION FOR FULL-DUPLEX RADIO

Master's Thesis

Supervisor: Yannick Le Moullec
PhD

Tallinn 2020

TALLINNA TEHNIKAÜLIKOOL
Infotehnoloogia teaduskond

Ritu Rani, 184605IVEM

TARKVARARAADIO PÕHINE DIGITAALSE ENESEHÄIRETE SUMMUTAMINE TÄISDUPLEKS-RAADIOLE

Magistritöö

Juhendaja: Yannick Le Moullec
PhD

Tallinn 2020

Author’s declaration of originality

I hereby certify that I am the sole author of this thesis. All the used materials, references to the literature and the work of others have been referred to. This thesis has not been presented for examination anywhere else.

Author: Ritu Rani

04.05.2020

Abstract

In the contemporary era, radio spectrum scarcity has become a pivotal problem in the field of telecommunication because of the unprecedented surge in the number of spectrum users. Coping with limited spectrum availability is a major challenge for future wireless systems. Full-Duplex (FD) radio is an emerging technology that allows wireless users to transmit and receive data simultaneously with the same frequency, which eventually improves the spectral efficiency and throughput of the system.

However, the main limiting factor for achieving FD is the self-interference problem which occurs due to presence of the strong transmit signal as compared to the desired received signal at the receiving node. This strong transmit signal acts as an interference to the desired received signal. This self-interference can be eliminated by using antenna cancellation, analog cancellation and digital cancellation techniques. This thesis mainly focuses on self-interference cancellation in the digital domain.

In this thesis the following work has been carried out; 1) performance evaluation of three adaptive algorithms, i.e., Least Mean Square, Normalized Least Mean Square and Recursive Least Square for digital self-interference cancellation, 2) design and Software Defined Radio based pseudo real-time implementation of digital self-interference cancellation.

The simulation results are evaluated by defining figures of merits such as amount of self-interference cancellation and mean square error. The pseudo real-time implementation is carried out for three cases: simulations only with realistic parameters, with RF cable, and over the air with antennas. A maximum amount of 31 dB of digital self-interference cancellation is achieved by simulation, and up to 20 dB and up to 8 dB with the RF cable and over the air, respectively.

This thesis is written in English and is 93 pages long, including 7 chapters, 34 figures and 10 tables.

Annotatsioon

Tarkvararaadio põhine digitaalse enesehäirete summutamine täisdupleks-raadiole

Kaasajal on raadiospektri nappus muutunud telekommunikatsiooni valdkonnas keskseks probleemiks, kuna spektri kasutajate arv on ennenägematult suurenenud. Piiratud spektri kättesaadavusega toimetulek on tulevaste traadita süsteemide peamine väljakutse. Täisdupleksne (FD) raadio on kujunemisjärgus tehnoloogia, mis võimaldab traadita kasutajatel edastada ja vastu võtta andmeid samaaegselt samal sagedusel, mis parandab lõpuks süsteemi spektraalset efektiivsust ja läbilaskevõimet.

FD-režiimi saavutamise peamiseks piiravaks teguriks on siiski enesehäirete probleem, mis ilmneb tugeva edastussignaali tõttu, võrreldes soovitud vastuvõetud signaaliga vastuvõtvas sõlmes. See tugev edastussignaal häirib soovitud vastuvõetud signaali. Selliseid enesehäireid saab kõrvaldada, kasutades summutamise tehnoloogiat antennis, analoog- või digitaalosas. See töö keskendub peamiselt enesehäire summutamisele digitaal-vallas.

Selles töös on tehtud järgmist: 1) kolme adaptiivse algoritmi (vähimruutude, normaliseeritud vähimruutude ja rekursiivse vähimruutude) jõudluse hindamine digitaalse enesehäirete summutamiseks, 2) disaini ja tarkvaraga määratletud raadiosidepõhine pseudo-reaalajas digitaalse enesehäirete summutamise rakendamine.

Simulatsiooni tulemusi hinnatakse, määratledes eeliste arvu, näiteks enesehäirete summutamise summa ja keskmise ruutvea abil. Pseudo-reaalajas rakendamine on teostatud kolme juhu osas: simulatsioonid ainult realistlike parameetritega; RF-kaabli abil ja raadio kaudu (antennide abil). Simuleerimise teel saavutatakse maksimaalne 31 dB digitaalsete enesehäirete summutamine ning vastavalt kuni 20 dB ja kuni 8 dB raadiosageduskaabli ja raadioside kaudu. Lõputöö on kirjutatud inglise keeles ning sisaldab teksti 93 leheküljel, 7 peatükki, 34 joonist, 10 tabelit.

List of abbreviations and terms

ADC	Analog to Digital Converter
AFC	Automatic Frequency Control
BER	Bit Error Rate
BS	Base Station
BSS	Blind Source Separation
DAC	Digital to Analog Converter
ENOB	Effective Number of Bits
EVM	Error Vector Magnitude
FD	Full-Duplex
FDD	Frequency Division Duplex
FD-R	Frequency Domain-Reconstruction
FPGA	Field-Programmable Gate Array
FPRF	Field-programmable RF
GRC	GNU Radio Companion
HD	Half-Duplex
ICA	Independent Component Analysis
IQ	In phase – Quadrature
LMS	Least Mean Square
LNA	Low Noise Amplifier
LO	Local Oscillator
LOS	Line of Sight
LTE	Long Term Evolution
MMSE	Minimum Mean Square Error
MSE	Mean Square Error
NLMS	Normalized Least Mean Square
NLOS	Non-Line of Sight

PA	Power Amplifier
RF	Radio Frequency
RLS	Recursive Least Squares
RMS	Root Mean Square
SDR	Software Defined Radio
SI	Self-Interference
SIC	Self-Interference Cancellation
SIR	Signal to Residual Interference Ratio
SINR	Signal to Interference and Noise Ratio
SNR	Signal to Noise Ratio
TDD	Time Division Duplex
TD-R	Time Domain-Reconstruction
ZF	Zero Forcing

Table of contents

List of figures

List of tables

1 Introduction

In the contemporary era, radio spectrum scarcity has become a pivotal problem in the field of telecommunication because of the unprecedented surge in the number of spectrum users. This number of users is increasing day by day; at the same time some bands are allocated to operators which are not actively used. So, limited spectrum is available for all the users. Coping with limited spectrum availability is a major challenge for future wireless systems. One significant inadequacy of the currently deployed systems is to operate as half-duplex systems utilizing either a time division duplex (TDD) or frequency division duplex (FDD) approach to enable bidirectional communication. Half-duplex transmission divides the spectral resources in time or frequency, which limits the systems to achieve two folds or two times spectral efficiency. But this limitation can be overcome by full-duplex systems where simultaneous bidirectional communication is carried out over the same spectral resources.

Full-Duplex (FD) radio is an emerging technology that allows wireless users to transmit and receive data simultaneously with the same frequency, which eventually improves the spectral efficiency and throughput of the system. Theoretically, this approach offers the benefit of increasing spectral efficiency by two folds.

This technology has a wide area of applications such as in 5G, military communication, tactical communication networks, civilian security etc. [1]. For instance, it solves the hidden node problem where recipient node utilizes the FD technology of simultaneous transmission and reception to acknowledge the reception and also inform the other nodes about the ongoing communication. So, this technology helps avoiding the collision between the nodes [2].

However, FD is not without its own challenges. Figure 1.1 reflects the major problem of self-interference (SI) signal while implementing a FD radio.

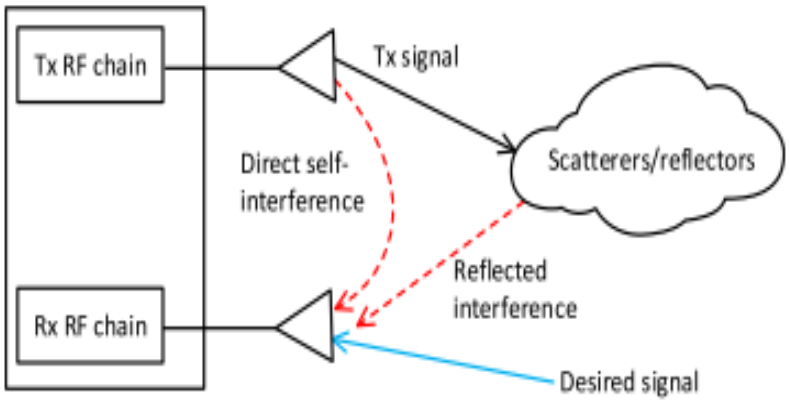

Figure 1.1. Concept illustration of a Full-duplex system [3]

In this FD system, where transmission and reception take place simultaneously on the same frequency, the transceiver experiences co-channel interference from its own transmitter known as direct SI signal. Usually the magnitude of the direct SI signal is higher than that of the desired signal which is transmitted by another transceiver. The transmitted direct SI signal is known to the receiver and can be subtracted from the received signal. However, as can be seen in the figure, the received total SI signal includes an additional component, namely the reflected interference which is affected by the propagation channel as well as by the transmitter and receiver impairments, which makes it different from the known transmitted signal.

This self-interference limits the performance of the FD radio, which should be mitigated with reliable methods grouped under the term self-interference cancellation. A typical FD system has three different cancellation stages, namely antenna cancellation, analog cancellation and digital cancellation stage; these are explained later in Chapter 2.

To implement a FD system, the most two popular architectures of FD designs are Stanford University design and Rice University design which are explained below.

For a long time, the practical implementation of a full-duplex radio system was looking impossible. However, researchers of Stanford University were among the first ones to present a full-duplex transceiver architecture in [4]. They used adaptive radio frequency (RF) filters before the low-noise amplifier (LNA) and subtracts the SI signal at the output of the LNA.

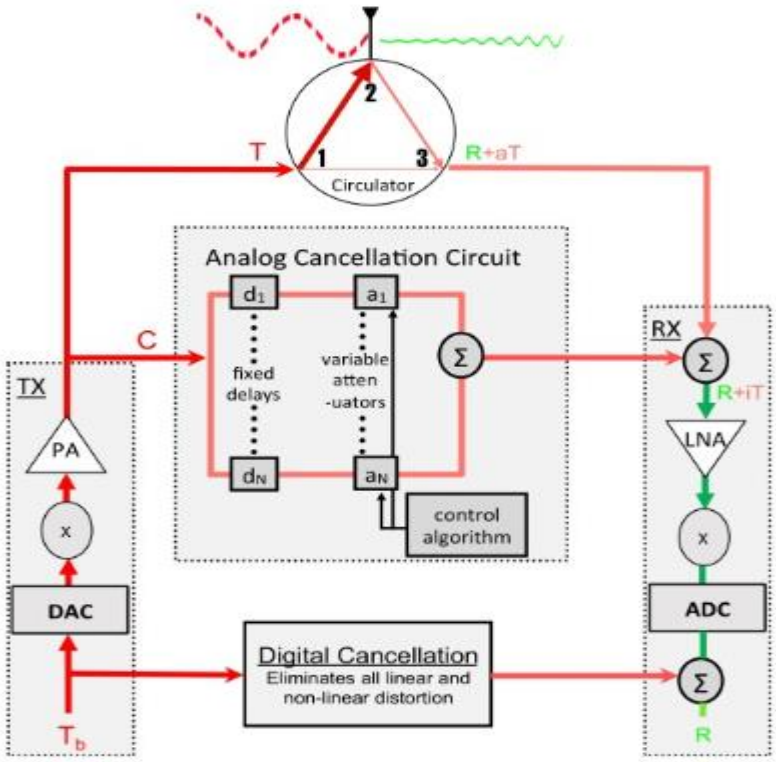

Figure 1.2. Full-Duplex Radio architecture proposed by Stanford University [4]

Figure 1.2 shows the architecture of the full-duplex radio which was proposed by Stanford University. Here, R (green colour) is the received signal whereas T (red colour) is the transmitted signal. The novelty of this architecture is the circuit and algorithms implementation and their good performance. According to authors' best knowledge, this hybrid cancellation technique is able to achieve 110 dB of SI cancellation. The main advantages of this architecture are that, it is used for wideband cancellation (80 MHz) and provides best cancellation till date. On the flip side, it requires a bulky board and analog cancellation tuned to few fixed delays/paths only [4]. Another popular FD transceiver architecture was proposed by the researcher of Rice University [5]. They used an additional digital transmission chain with the same RF chip of Stanford design. The implementation of this architecture is simple and includes baseband processing. It provides low cancellation for narrowband signals (625 kHz) and requires three RF chains. The upper part of Figure 2.2 in Chapter 2 shows the architecture of full-duplex radio proposed by Rice University.

These above mentioned two architectures have been widely used for the implementation of FD transceiver and proves the practical feasibility of the FD concept.

1.1 Motivation to study FD Radio

A FD radio is an enabling technology which can solves the problem of spectrum scarcity and increases the spectral efficiency by two folds which is highly desirable. Moreover, it has wide practical applicability such as in military communication, cognitive networks, solving the hidden node problem, civilian security and tactical communication networks etc.

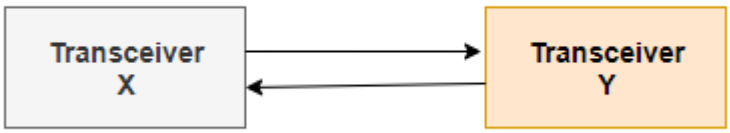

Figure 1.3. Point to point communication link of full-duplex system

A point-to-point communication link of FD system is shown in Figure 1.3. According to Shannon, the capacity formula for a half-duplex system in [6] can be expressed as

$$C_{HD} = B\ log_2\ (1 + SNR) \tag{1.1}$$

Here, C_{HD} is the capacity for a half-duplex system in bits per second, B is bandwidth in Hertz, and SNR is the signal to noise ratio. Equation 1.1 depicts the capacity of the half-duplex system.

For an ideal full-duplex system, let us assume the SI signal is completely cancelled while maintaining constant SNR; the capacity of the FD radio, C_{FD}, can be expressed as [6];

$$C_{FD} = Blog_2\ \left(1 + SNR_{X,Y}\right) + Blog_2\ \left(1 + SNR_{Y,X}\right) \tag{1.2}$$

Here, $SNR_{X,Y}$ and $SNR_{Y,X}$ are the signal to noise ratios at the receiving ends in the FD system.

Let us consider the SNR is equal in both directions, therefore Equation 1.2 becomes [6]

$$C_{FD} = Blog_2\ (1 + SNR_{FD}) \tag{1.3}$$

It can be seen from Equations 1.1 and 1.3 that the spectral efficiency is twofold in a FD system as compared to a HD system. It is critical to achieve the same signal to noise ratios in a FD system to double the capacity.

The biggest challenge to implement this emerging technology is the SI cancellation. These SI cancellation techniques can be characterized by three main factors, namely cancellation capability, computational complexity, and applicability region [7]. There is always a trade-off between these three factors. For example, SI cancellation techniques with large antenna separation cannot be used for mobile applications. For instance, conventional digital SI cancellation techniques are the least complex but more applicable, but their cancellation capability is very limited (30-40 dB). On the flip side, a significant amount of SI cancellation could be achieved by using analog SI cancellation technique, but this increases the complexity and has limited applicability. In a nutshell, a good SI cancellation technique should have wide application range, significant cancellation capability and low complexity. Such challenging requirements are the main motivation behind the work in this thesis and the main focus is on digital SI cancellation technique.

1.2 Application of Full-Duplex Radio

1.2.1 Resolve the Hidden Node Problem

The hidden node problem is a most critical issue in mobile ad hoc networks. Let us consider three node networks where the central node can access other two nodes, but they are unaware of each other. These unaware (hidden) nodes can try to communicate with the central node which results in a collision. In this scenario, if the FD system is applicable at the central node, then this collision could be avoided by sending a “busy” signal while receiving from any other node. This can be main benefit of using FD system in medium access control layer, as this technique reduces the number of collisions and eventually increases the throughput [2].

1.2.2 Cognitive Radio Networks

Cognitive radio networks are smart networks in terms of spectrum sensing, sharing and management. A cognitive radio assigns the unused spectrum (spectrum hole) to the secondary user as long as primary user does not use it. FD technology could help to avoid the collision between the primary and secondary users [2].

1.2.3 Full Duplex Base Station

A base station (BS) serves a number of users by using FDD or TDD mode. If this BS operates in FD mode, then it can serve two users at a same time. For instance, a BS can serve a transmitting mobile user and a receiving mobile user at same time, but spatial separation should be used to avoid the inter user interference [1].

1.2.4 Military Communication

Military radios should have robustness, low detection probability, and good jamming resistance. These requirements could be fulfilled using the FD technology. With FD technology, simultaneous communication and jamming, and simultaneous interception and jamming is possible. Moreover, for simultaneous interception and communication, devices that perform spectrum monitoring and signal surveillance could transmit the gathered information to the tactical units without compromising the surveillance capabilities during transmission [1].

1.2.5 Civilian Security

FD technology could be used to prevent the unauthorized use of remotely controlled unmanned aerial vehicles near restricted areas by using a protective electromagnetic field called “radio shield”. This radio shield is created by jamming signals and prevents the unknown party from receiving the wireless transmissions [1].

FD is also an emerging technology for the Internet of Things which allows power transfer and communication with sensors remotely and securely. In addition, FD radio shield provides encryption in the implanted medical devices for secure communication [1].

1.3 Research Statement

The most challenging aspect to be considered for the implementation of a FD system is efficient and sufficient cancellation of SI caused by the transmitter, multipath reflections, linear and nonlinear components, noise floor, and ADC quantization noise.

Digital SI cancellation (SIC) is the last step to safeguard against self-interference and to bring the SNR to the desired level. For example [7], as shown in Figure 1.4, assumes that the transmitted power of a Wi-Fi signal is 20 dBm, the receiver noise floor is approximately -90 dBm, and highest level of the desired signal is -70 dBm. This means that in order to extract the desired signal, 110 dB of SI signal should be cancelled.

Assume that 50-60dB of SI mitigation is achieved by analog cancellation. So, the residual 50 dB interference should be eliminated by the digital SIC. But a major limiting factor is the dynamic range of the ADC. Digital SI canceller can suppress SI only up to effective ADC dynamic range. Mostly, in the Wi-Fi radios, a 12-bit ADC with 10 bits ENOB is implemented, which provides an effective dynamic range of 60 dB. So, the maximum input signal at the receiver end is -30 dBm. Therefore, analog cancellation should be large enough to avoid reaching the receiver's saturation point.

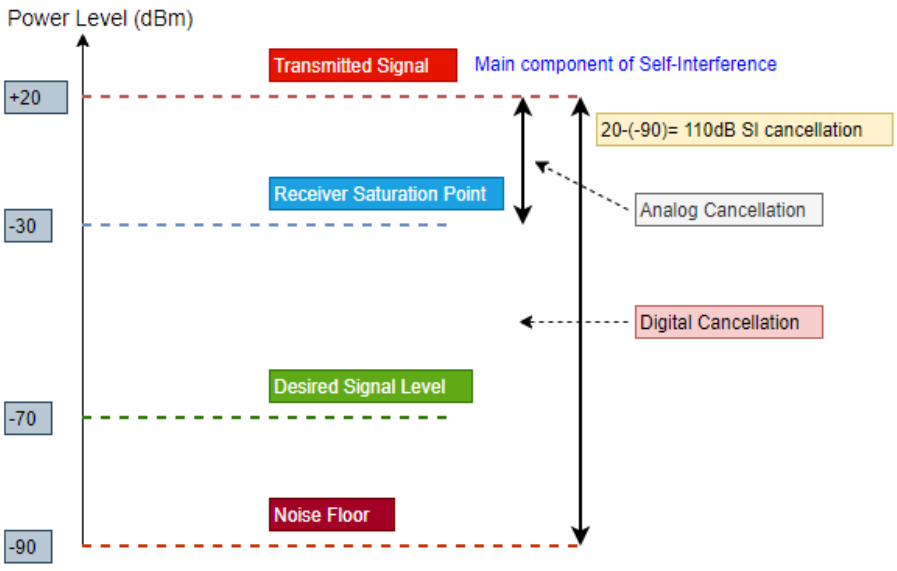

Figure 1.4. Illustration of requirements of digital cancellation process for Wi-Fi signals

There is a limited number of practical implementations of FD systems, especially based on flexible software defined radios, documented in the scientific literature. Thus, there

is need for better understanding and evaluating the possible performance of digital SIC using such platform.

In this thesis, the main aim is to evaluate possible amount of SI cancellation by mitigating the linear components of SI using an efficient algorithm in the **digital domain.** In addition, this thesis also explores how to implement a pseudo real-time FD system and analyses the different factors which affects the digital SIC process.

Given the above, the research statement of this thesis work is as follows:

- **Analyze the performance of different algorithms (LMS, NLMS and RLS) for key figures of merits (amount of SI cancellation, mean square error) for digital SIC process for FD system.**
- **Implement a practical realization of pseudo real-time FD system and analyze the influence of key factors on its performance.**

1.4 Approach Followed in This Thesis

The following steps have been taken to accomplish the goal of this thesis.

- Get an understanding of the FD wireless radio and surveying the SIC techniques.
- Perform SI channel modeling by understanding the main parameters of the channels and their effect (Rician and Rayleigh fading channels).
- Analyze the performance of the algorithms least mean square (LMS), normalized least mean square (NLMS) and recursive least square (RLS) by means of simulations and compare their performance according to the figures of merit that will be defined.
- Practical implementation of pseudo real-time FD system by considering three different cases such as with simulation, transmission/reception using RF cable and transmission/reception over the air.
- Digital SIC is performed in offline mode with LMS algorithm and a comparative analysis is performed by considering the achieved amount of digital SIC.

- Evaluation of different factors such as step size, estimation filter length, number of samples which affects the amount of digital SIC.

This thesis is organized as follows. Chapter 2 gives an overview of self-interference cancellation techniques available in the scientific literature. Next, Chapter 3 discusses the digital self-interference cancellation process and theoretical background of adaptive filter algorithms, namely LMS, NLMS and RLS. It also shows some simulation results of these adaptive algorithms. Chapter 4 presents various wireless channel models and SI channel modelling briefly with some simulation results. Chapter 5 discusses the experimental set up, simulation model, and implementation model for the pseudo real-time implementation of FD system. Simulation and implementation results are presented and discussed in Chapter 6. Chapter 7 presents the conclusion and future work. The thesis ends with the list of references and appendices.

2 State-of-the-Art on Self-Interference Cancellation Techniques for Full-Duplex Radio

This chapter represents the research work on different self-interference cancellation techniques published in the scientific literature. Generally, these techniques are categorized into two main types, known as *passive and active cancellation.* A full-duplex system needs both passive suppression and active cancellation for achieving a significant amount of SI cancellation. In the literature, various authors have proposed active, passive and hybrids of both cancellation types to reduce the self-interference signal level [5][4][8][9]. A high-level of classification of SIC techniques is shown in Figure 2.1.

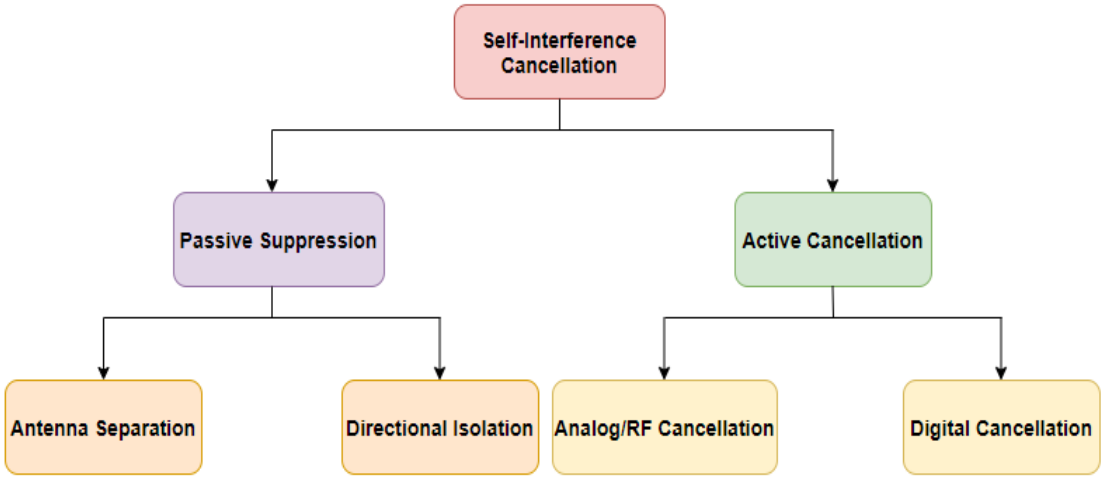

Figure 2.1. High-level classification of SIC Techniques

Figure 2.2 depicts the most popular FD radio architecture [1], the upper part shows the architecture proposed by Rice university and the lower part shows the architecture proposed by Stanford University. The general description of these two architectures was given in Chapter 1. In this Chapter 2, these architectures are used to elaborate the three different types of SI cancellation techniques. In Figure 2.2, the architectures are divided

into three different sections, namely passive suppression, analog cancellation, and digital cancellation.

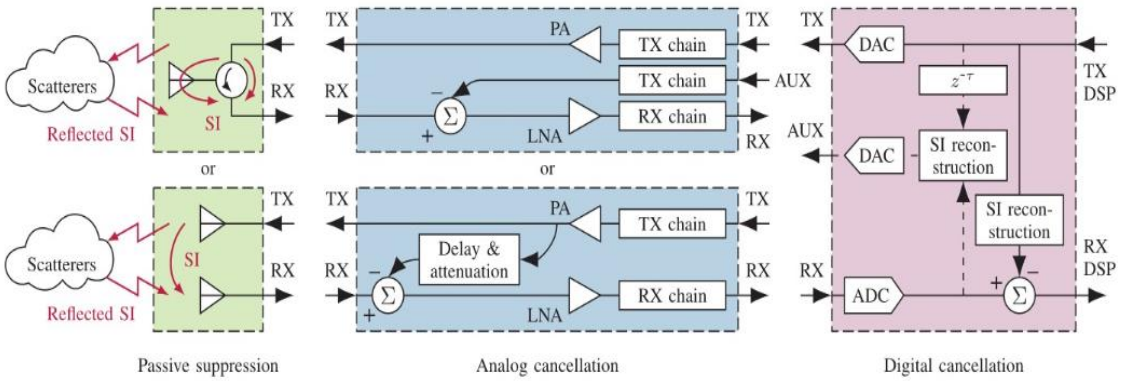

Figure 2.2. The most popular Full-Duplex Radio Architectures [1], the upper part shows the architecture proposed by Rice university and the lower part shows the architecture proposed by Stanford University

In passive suppression techniques, the SI signal is suppressed in the propagation domain prior it is processed by the receiver. This can be achieved by antenna separation or directional isolation. Active cancellation techniques (analog and digital cancellation) rely on the fact that receiver knows the transmitting signal and later the SI signal is mitigated by subtracting a copy of the known transmitting signal from the received signal.

In the first architecture (upper part of Figure 2.2), the reference signal for the RF stage is taken from the output of the power amplifier (PA) whereas the second architecture (lower part of Figure 2.2) takes the reference signal for both RF and baseband from the output of the PA. The output of the PA is used to cancel the SI signal. This signal is passed through the parallel varying delay lines and tuneable attenuators lines. After passing these lines, a copy of the received SI signal is obtained and eventually the obtained signal is subtracted from the received signal. Space limitation and power consumption are the limiting factor for multipath SI channel because for this, a large number of delay lines are needed.

2.1 Passive Suppression Techniques

In the passive suppression technique, the SI signal is suppressed by antenna separation or directional isolation. The amount of SI signal suppression in this technique highly depends on the application and physical constraints of the specific system. For instance, in devices with small dimensions such as mobile applications, the amount passive suppression is very limited by using antenna separation and isolation method. On the flip side, for a radio relay system, these methods can provide significant passive suppression. For this, physical separation between the transmitter and receiver antennas mechanism is used [5]. For example, 75-90 dB of passive suppression is achieved by using directional isolation and antenna separation (4-5 m) [10] .

The authors in [4] proposed a passive suppression technique of separate antennas for transmission and reception (50 cm distance), absorptive shielding and cross-polarized antennas and achieved 74 dB of interference suppression. Additionally, concatenation of active RF and passive suppression is able to achieve 95 dB cancellation for 20 MHz bandwidth [5]. Reflected paths are the limiting factor of passive suppression which are not possible to suppress passively and require active cancellation.

2.2 Active Cancellation Techniques

Active cancellation is mainly categorized into two types named analog and digital cancellation based on the signal domain (analog or digital) where the SI signal is actively cancelled.

2.2.1 Analog Cancellation

Analog cancellation technique cancels the SI signal by adding a phase inverted analog signal in the RF domain and the cancellation signal is generated by SI channel estimation. In Figure 2.2, two different techniques available for active analog cancellation are shown.

The mechanism of the first technique is to split the amplified signal before transmission and use a modified version of the replica to subtract from the SI signal. Another technique uses an auxiliary transmitter chain and a separate signal which is generated for subtracting it from the SI signal. The former technique has the advantage that the transmitter’s imperfections are included in the signal which is subtracted from the

received signal whereas in the latter technique these imperfections should be modelled and applied to the generated replica [1].

For a single antenna system with circulator, wideband (80 MHz bandwidth), analog cancellation is implemented by means of dynamic adaptation of delays and attenuators which able to achieve 60 dB SI cancellation [4]. Antenna cancellation, pre-nulling, automatic frequency control (AFC), pre-coding/decoding, block diagonalization, zero forcing (ZF) filters, optimal Eigen beamforming and minimum mean square error (MMSE) filtering are popular algorithms which are used for analog cancellation [11]. The main benefit of analog cancellation compared to the digital one is that it prevents the receiver from being saturated due to high SI signal power because the SI signal is cancelled in the analog domain before the signal goes through the receiver RF circuitry.

2.2.2 Digital Cancellation

Digital cancellation techniques are used to cancel the remaining SI after analog cancellation. The process involves the reconstruction of the SI signal by predicting the known transmitting symbols inside the receiver where the cancellation is performed, as illustrated in Figure 2.3.

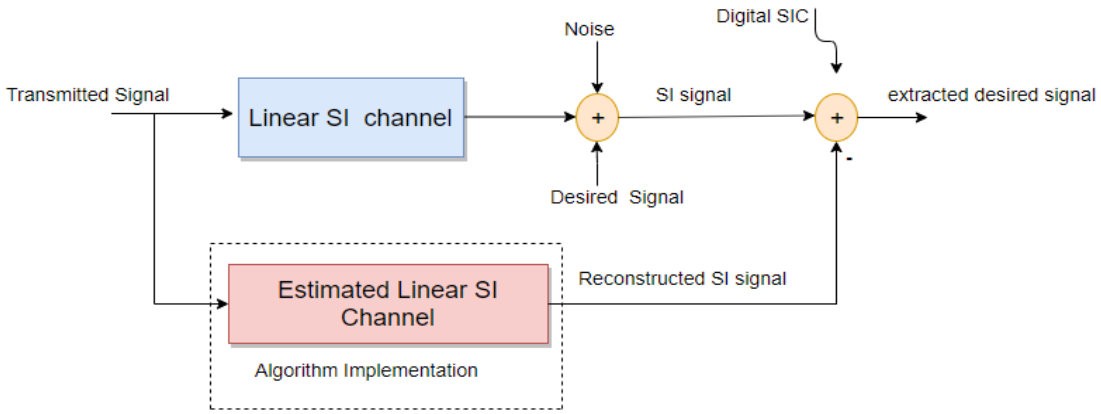

Figure 2.3. A generalized block diagram of digital SIC process

Digital SIC is a technique which cancels the SI at the baseband level. The SI signal is generated when the baseband transmitted signal passes through the linear SI channel, and noise and the desired signal are superimposed on the transmitted signal. Here, the linear SI channel can be modelled as a Rayleigh or Rician fading channel. Estimated SI channel can be implemented using different algorithms such as LMS, NLMS and RLS.

Digital SIC is performed by subtracting the SI channel signal and estimated SI signal to calculate the amount of cancellation.

A typical full-duplex system can be implemented by using all of the three techniques to achieve a desired SI cancellation amount of signal. In the literature, some authors have proposed this system. For instance, in [8], a digital cancellation scheme is used to supplement RF/Analog cancellation technique. The precision of digital SIC is limited by the PA nonlinearity and transmit in phase/quadrature (I/Q) imbalance. They proposed a two-stage iterative self-interference cancellation scheme based on the power amplifier output signal to improve the output signal to interference and noise ratio (SINR). In the first stage, 46 dB of cancellation is achieved when the transmitter and the receiver isolation is 40 dB. Moreover, the cancellation amount increased to 60-70 dB for the same isolation amount of 40 dB between transmitter and receiver in the second stage. Only 28 dB of cancellation achieved by digital cancellation technique and the main impediments are quantization error and phase noise which are hard to handle by digital cancellation technique [8].

In [4], a real-time full duplex radio is prototyped by combining a dual-polarization antenna-based analog part with a digital self-interference canceller that operates in real time. This prototype is based on the LTE downlink standards and implemented using LabVIEW system design software and the state-of-the-art PXIe SDR platform. The dual-polarization antenna provides about 42 dB isolation and 18 dB of analog self-interference cancellation is achieved by tuning the attenuation, phase shift, and delay parameters. In the digital domain, the error vector magnitude (EVM) is calculated to measure the self-interference cancellation (43 dB). Eventually, a total 103 dB of SI cancellation is achieved by using this prototype [4].

A digital SI cancellation scheme was presented in [7] where an auxiliary receiver chain was used to obtain a digital-domain copy of the transmitted RF SI signal. This copied signal was used to cancel out the SI signal in digital domain. The proposed technique significantly mitigates the transmitter impairments such as receiver phase noise and nonlinearity effects. The achieved level of the SI signal is approximately 3 dB higher than the receiver noise floor. Eventually, for 20 dBm of transmit power, the proposed FD system is able to achieve 67-76% rate improvement as compared to conventional half-duplex systems. The proposed system has a two-antenna transceiver architecture,

where the amount of passive suppression will be limited by the circular coupling (approximately 20 dB). The main limitation of this proposed system is that, it is not applicable for low transmit power applications (5 dB) when a circulator is used because it saturates the receiver RF circuitry [7].

Computational complexity is a limiting factor for the implementation of digital SIC technique. In [12], a linear digital SIC approach is used to computational complexity where SI signal is reconstructed with frequency domain-based approach in digital domain. This proposed approach reduced the computational complexity by 61% as compare to time domain reconstruction. The simulation results demonstrated that the proposed frequency domain-reconstruction (FD-R) approach is not only comparable with the time domain-reconstruction (TD-R) but, it can offer 5−7 dB better cancellation under selective fading conditions than existing approach. This approach is suitable for long range transmissions. For outdoor application, the FD approach is limited because the performance of the digital cancellation degraded with the larger values of RMS delay spreads [12].

It is known that IQ imbalance and PA non-linearity limit the amount of achievable SI cancellation amount. Thus, a joint digital SIC scheme was proposed in [13] with consideration of IQ imbalance and PA non-linearity for a 16 QAM based FD system. This joint cancellation scheme not only eliminates the PA nonlinear components and the image components, but the mixed components of these two non-linear components. The achieved SI cancellation was 108 dB by eliminating all the distortions caused by IQ imbalance and PA non-linearity. This scheme was able to suppress the SI to the next significant noise component, or the amount of residual SI is very minimum. It provides a good amount of SI cancellation (108 dB) but increases in the complexity of the model is the main drawback of this joint digital canceller [13].
Table 2.1 summarizes the overall state-of-the-art SI cancellation techniques. Table 2.2 presents further details of notable works.

Table 2.1. Summarized State-of-the-Art of SI cancellation

Year of publication	Author	Title	Remarks
2013	Evan Everett, Achaleshwar Sahai, and Ashutosh Sabharwal	Passive Self-Interference Suppression for Full-Duplex Infrastructure Nodes	In [5], author proposed a passive suppression technique of separate antennas for transmission and reception (50 cm distance), absorptive shielding and cross-polarized antennas and achieved 74 dB of interference suppression. Concatenation of Active RF and passive suppression achieved 95 dB cancellation for 20 MHz bandwidth.
2013 Computer Communication Review	D. Bharadia, S. McMilin and S. Katti	Full Duplex Radios	In [4], a single antenna system with circulator, wideband (80 MHz bandwidth), Analog cancellation implemented by means of dynamic adaptation of delays and attenuators (60 dB) with Digital cancellation (50 dB).
2014	Shenghong Li,	An Investigation	In [8], a digital

IEEE Transactions on Wireless Communication	Student Member, IEEE, and Ross D. Murch, Fellow, IEEE	into Baseband Techniques for Single-Channel Full-Duplex Wireless Communication Systems	cancellation scheme is used to supplement RF/Analog cancellation technique. Authors 'proposed a two-stage iterative SIC scheme based on the power amplifier output signal to improve the output SINR (Signal to Interference and Noise Ratio). 46 dB cancellation is achieved in first stage with 40 dB of isolation, the cancellation increases to 60-70 dB in second stage for the same isolation.
2015 (IEEE Magzine)	MinKeun Chung, Min Soo Sim, Jaeweon Kim, Dong Ku Kim, and Chan-Byoung Chae	Prototyping Real-Time Full Duplex Radios	In [9], a real-time full duplex radio is prototyped by combining a dual-polarization antenna-based analog part with a digital self-interference canceler that operates in real time. Dual-polarization antenna provides about 42 dB isolation and 18

			dB of analog SIC is achieved by tuning the attenuation, phase shift, and delay parameters. In the digital domain, error vector magnitude (EVM) is calculated to measure the self-interference cancellation (43 dB).
2015 IEEE Transactions on Wireless Communication	Elsayed Ahmed and Ahmed M. Eltawil, Senior Member, IEEE	All-Digital Self-Interference Cancellation Technique for Full-Duplex Systems	In [7], a novel digital SIC scheme, where an auxiliary receiver chain was used to obtain a digital-domain copy of the transmitted RF SI signal. This copied signal was used to cancel out the SI signal in digital domain The achieved level of the SI signal is approximately 3 dB higher than the receiver noise floor. Eventually, for 20 dBm of transmit power, the proposed FD system is able to achieve 67-76% rate improvement as compared to conventional half-

			duplex systems.
2017 IEEE Wireless Communication and Networking	Muhammad Sohaib Amjad, Ozgur Gurbuz	Linear Digital Cancellation with Reduced Computational Complexity for Full-Duplex Radios	In [12], SI signal was reconstructed with frequency domain-based approach in digital domain. This proposed approach reduced the computational complexity by 61% as compare to TD-R. FD-R approach can offer 5−7 dB better cancellation under selective fading conditions than existing approach.
2017 IEEE Access	Jiong Li, Hang Zhang, and Menglan Fan	Digital Self-Interference Cancellation Based on Independent Component Analysis for Co-Time Co-frequency Full-Duplex Communication Systems	In [14], two SIC algorithms have been proposed based on independent component analysis (ICA). Problem of LOS component of SI was solved with auxiliary chain receiver and reference signal. ICA- BSS (Blind Source Separation) was used to solve the problem of multipath SI channel. This proposed approach

			able to achieve 6 dB more gain compared with LS-based approach.
2017 Conference Record-Asilomar Conference on Signals, Systems and Computers	Dani Korpi, Mona AghababaeeTafreshi, Mauno Piilil¨a, Lauri Anttila, and Mikko Valkama	Advanced Architectures for Self-interference Cancellation in Full-duplex Radios: Algorithms and Measurements	In [15], a real-time nonlinear digital SI canceller using LMS algorithm is implemented on a FPGA. 90 dB of SI is cancelled by the integrated RF and digital SI canceller. The main limitation of real time digital canceller is the low transmit power (0-10 dBm) which can only suppress 25-35 dB. The modelling accuracy of the digital canceller should be improved for higher transmit powers.
2018 Journal of Signal Processing Systems	Mona Aghababaeetafreshi, Dani Korpi, Matias Koskela, Pekka Jaaskel ainen, Mikko Valkama, Jarmo Takala	Software Defined Radio Implementation of a Digital Self-interference Cancellation Method for In band Full-Duplex	In [16], for mobile-scale devices, a nonlinear digital SI canceller is implemented using an adaptive cancellation algorithm. The proposed digital

		Radio Using Mobile Processors	canceller is implemented for 20 MHz LTE band. This canceller cancels the SI signal approximately close to the receiver noise floor (-90 dBm). Third order non-linear SI canceller outperforms the linear canceler. Slower convergence is the limiting factor to achieve the perfect SIC by using LMS algorithm.
2018 ITM Web of Conferences	Meijing Zhou, Nan Chen, Changhua Zhu, and Yunhui Yi	Joint Digital Self-Interference Cancellation in Full-duplex Radios under IQ Imbalance and Transmitter Non-linearity	In [13], a joint digital SIC with consideration of IQ imbalance and PA non-linearity for a 16 QAM based FD system. This scheme is capable to eliminate the mixed components of PA nonlinear components and the image components. It provides a good amount of SI cancellation (108 dB) but increase in the complexity of the model is the main

			drawback of this joint digital canceller.
2019 Elsevier	Mikail Yilan, Ozgur Gurbuz, Huseyin Ozkan	Nonlinear digital self-interference cancellation for full duplex communication	In [17], a digital nonlinear cancellation integrated with linear cancellation was proposed to enhance the performance of FD radios. Integration of these two techniques with single antenna FD radio set-up, achieved 5 dB improvement in the cancellation performance for the existing system without additional hardware cost, unlike the existing works.

Note: While reviewing the literature, the thesis' author also found some patents related to Full Duplex radio technology which comprised of demonstration of FD system for MIMO two-way relay channels [18], which proposed a representative example of analog cancellation circuitry for SI cancellation.

Table 2.2. Summarized table of the most notable above works

SI cancellation scheme	Bandwidth	SI cancellation	Reference
Separate antennas for transmission and reception (50 cm distance) + optional use of cross-polarized antennas + Active RF and	20 MHz	95 dB	[5]

BB cancellation			
Single antenna solution with circulator + Analog cancellation implemented by means of dynamic adaptation of delays and attenuators (60 dB) + Digital cancellation (50 dB)	80 MHz	110 dB	[4]
RF + Digital Cancellation - two-stage iterative SIC scheme -Consider PA and I/Q imbalance non-linearities	-	98 dB	[8]
SDR platform with dual polarized antenna +RF + Digital cancellation	20 MHz	103 dB	[9]
Balun + Digital cancellation	10-40 MHz	73 dB	[19]
Antenna cancellation + RF + Digital cancellation	5 MHz	60 dB	[20]
Separate antennas for transmission and reception (20 cm distance) + RF cancellation with additional RF chain + Digital base band (BB) interference cancellation	625 kHz	78 dB	[21]

2.3 RF Impairments

Digital SIC is applied after analog cancellation at baseband level to suppress the SI signal. The SI channel can be modelled as linear or nonlinear channel. Linear digital SIC estimates the channel using the known transmitted signal for reconstructing the replica of SI signal which is further subtracted from the received signal. Nonlinearity

comes in the picture at higher transmit powers where amount of linear SIC drops significantly because of nonlinear characteristics of the transceiver hardware. The main two nonlinear characteristics are PA nonlinearity and IQ imbalance.

2.3.1 IQ Imbalance

In practice, each component of the transceiver is considered as non-ideal and causes non-linearities in the system. IQ imbalance is a salient problem in the transceiver chains. The mismatch between the I and Q branches is the main cause of this IQ imbalance. Ideally, the quadrature modulator should have a constant gain and linear phase, the gain of the I and Q branches is equal and phase of the LO (Local Oscillator) signal is orthogonal [13]. In real-time, the practical circuits with quadrature modulator always have a certain amplitude and phase deviation which causes IQ imbalance and eventually creates mirror-frequency interference. So, it is important to consider this RF impairment to get better results for self-interference cancellation in FD system.

2.3.2 PA Non-linearity

The PA is a crucial component of the transmitter in communication system. When the PA is operated near to its saturation point to obtain maximum power efficiency, it creates non-linear distortion. PA efficiency and linearity are reciprocal to each other. However, nonlinear PAs are important to achieve maximum power efficiency but at the cost of non-linear distortion, adjacent channel interference which degrades the bit error rate (BER) performance [22]. In a nutshell, it is critical to consider these PA nonlinearities to increase the amount of SIC in FD system. In digital SIC, for reconstruction of SI signal, channel modelling should consider the PA nonlinearities.

3 Digital Self-Interference Cancellation

After applying analog cancellation, a digital SIC technique which cancels the residual SI at baseband level is applied. It is assumed that the receiver where the cancellation is being performed already knows the transmitted samples and has predicted a received SI. The received SI is combination of direct SI and reflected SI which is explained in Figure 1.1 in Chapter 1. In [23], a nonlinear digital cancellation technique along with RF cancellation is proposed which is modified for the linear digital cancellation in this thesis.

In [22], x_n is the original digital transmit signal. The impulse response of the linear SI channel is h_n whereas the impulse response of estimated SI channel is h'_n.The linear SI channel can be modelled as Rician or Rayleigh multipath fading channel because multipath exists between the transmitting and receiving antenna which introduce some fading in the transmitted signal. The estimated SI channel is modelled as a finite impulse response (FIR) filter which has L number of delays and the weight varies from w_o to w_{L-1}. Here, d_n is the desired signal at the receiving antenna, which gets superimposed with the SI signal and a_n is an additive white gaussian noise. Based on Figure 3.1, the total SI signal can be expressed as

$$x_n^{SI} = x_n \otimes h_n + d_n + a_n \tag{3.1}$$

On the other side, the known transmitted signal or reference signal is passed through the estimated SI channel and generate an estimated SI signal i.e. x'^{SI}_n which is used to cancel the SI signal and expressed as

$$x'^{SI}_n = x_n \otimes h'_n = \sum_{k=0}^{L-1} w_k \, x_{n-k} \tag{3.2}$$

Now, let us subtract the estimated SI signal from the SI signal, this is known as the digital SI cancellation process.

$$d'_n = x_n^{SI} - x'^{SI}_n \tag{3.3}$$

Here, d'_n is the signal received after digital cancellation. The estimated SI channel can be implemented using an adaptive estimation algorithm such as LMS, NLMS or RLS.

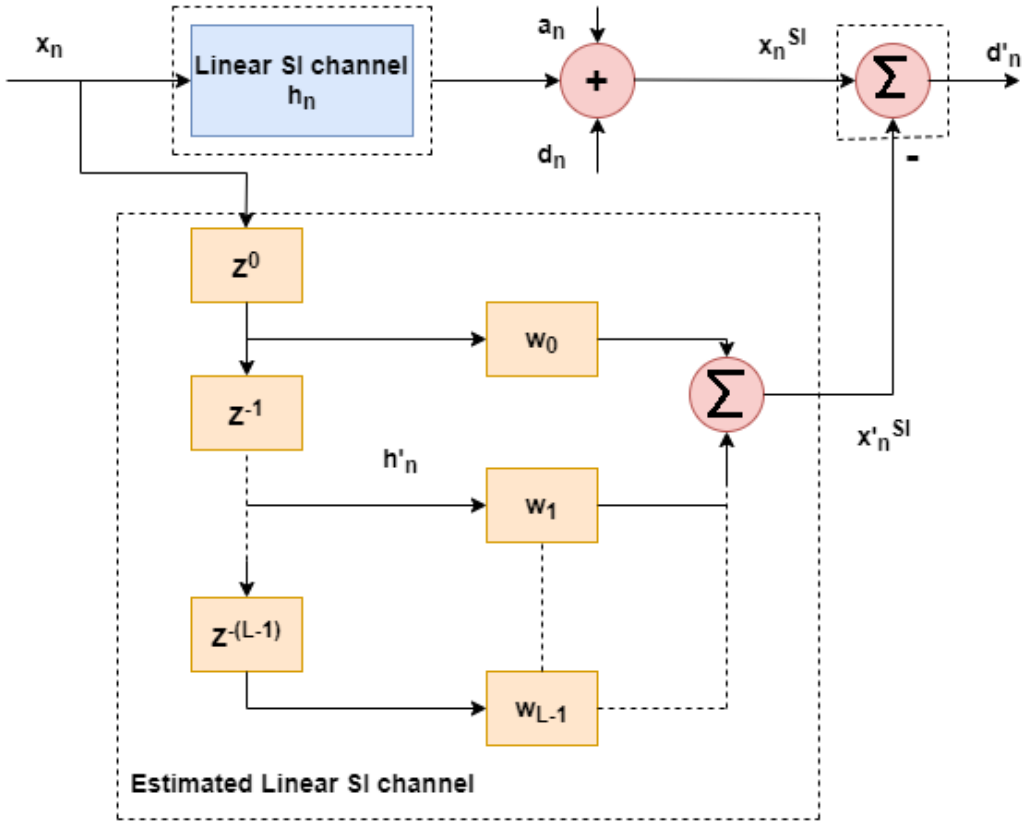

Figure 3.1. Digital SI cancellation technique, modified from [23]

In this thesis, a linear SI channel is modelled for the digital cancellation process which is not capable to mitigate the effect of the non-linearities such as PA noise and IQ imbalance introduced by the transceiver. This approach decreases the level of SI cancellation. However, it is possible to achieve a higher level of cancellation by mitigating the non-linearities effect. For good estimation, the length of the estimation filter should be long enough to minimize the error.

The next sections in this chapter discuss different adaptive filter algorithms, namely LMS, NLMS and RLS for SI cancellation.

3.1 Background of Least Mean Square Algorithm

An adaptive filter is a filter which operates by calculating the difference between the desired signal and the adaptive filter output. Figure 3.2 depicts a generalized block diagram of a FIR-based adaptive filter where w represents the coefficients of the filter tap weight, $x(n)$ is the input signal, $y(n)$ is the output of adaptive filter, z^{-1} represents unit delay, $d(n)$ is the desired signal and the error signal is represented by $e(n)$. The error signal is given as feedback into the filter and its coefficients are updated algorithmically to minimize the error [24].

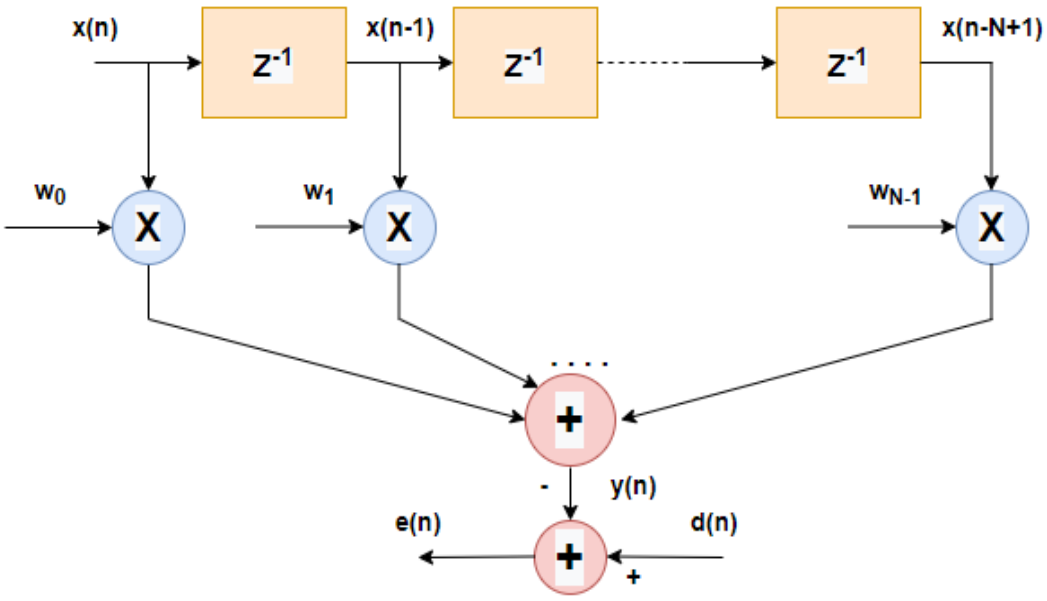

Figure 3.2. Generalized block diagram of a FIR-based adaptive filter, modified from [24]

The LMS filter is a linear adaptive filtering algorithm which is based on the steepest descent algorithm. It has vast applicability such as in channel equalization, echo cancellation and interference cancellation. This algorithm is widely used due to its computational simplicity.

Here, the estimation error is the difference of the desired signal and the adaptive filter output. The filter weights are updated by using this estimation error and these are updated until the mean square error is minimized.

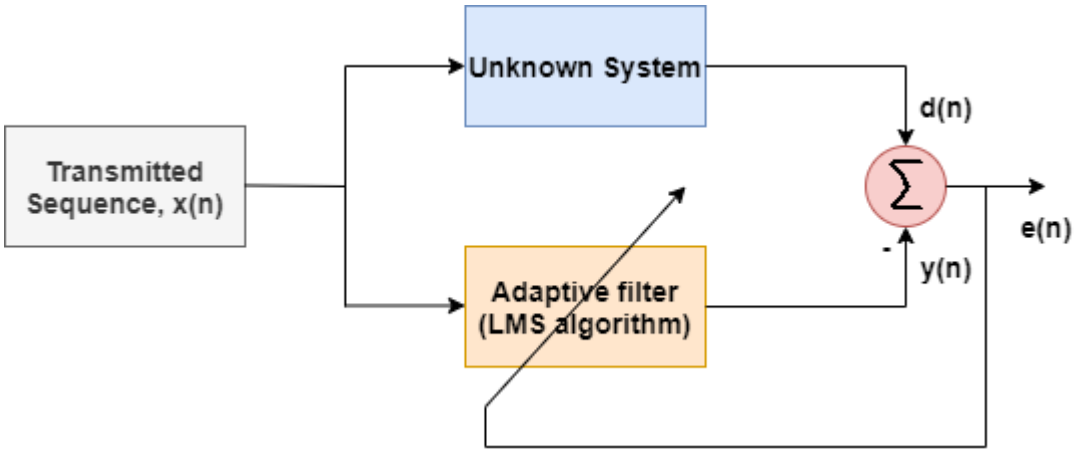

Figure 3.3. An adaptive filter for system identification

In Figure 3.3, a transmitted sequence $x(n)$ is generated which is passed through an unknown system, or channel, and produce an output signal called $d(n)$. This transmitted sequence $x(n)$ is also passed through an adaptive filter where the LMS algorithm estimates the unknown system, resulting in $y(n)$. This algorithm updates the weights of the filter in each iteration according to Equation 3.4 [25].

The output of the adaptive filter $y(n)$; is calculated as

$$y(n) = w^H(n)x(n) \tag{3.4}$$

An error signal is the difference between the desired signal and the adaptive filter output, which is given as

$$e(n) = d(n) - y(n) \tag{3.5}$$

The filter weights are updated for the next iteration according to the Equation 3.6,

$$w(n+1) = w(n) + \mu e(n)x(n) \tag{3.6}$$

where, $w(n)$ is the weight of the filter at sample n. For the weight updating processing, the initial weight has to be guessed. Generally, initial weights are initialized with zeroes.

In each iteration, this algorithm uses the current values of $x(n)$, $d(n)$ and $e(n)$ to update the new weight $w(n+1)$ of the filter.

The step size is the critical factor to control the convergence rate of the algorithm. The value of the step size should be calculated accurately to get good estimation results. The step size depends on the maximum value of power spectral density (PSD) of the tap inputs $x(n)$ and the filter length M, and this condition can be represented as in Equation 3.7 [18]

$$0 < \mu < \frac{2}{MS_{max}} \tag{3.7}$$

where S_{max} depicts the maximum value of the PSD of the tap inputs $x(n)$. It is known that the step size (μ) controls the influence of the update factor and this value should be chosen carefully. If this value is too small, then the convergence time will be too long whereas if it is too large then the output will become unstable and start to diverge instead of converging.

The main disadvantage of the LMS algorithm is its fixed step size for every iteration. This algorithm is not applicable where the input signal to the adaptive filter is non-stationary which requires a variable step size. But this limitation is overcome by the NLMS algorithm which is explained in the next section.

3.2 Background of Normalized Least Mean Square Algorithm

NLMS is an extension of the LMS algorithm which is capable to overcome the fixed step size drawback of the LMS algorithm. Indeed, the NLMS algorithm can provide variable step size for each iteration of the algorithm. The step size is inversely proportional to the inverse of the total expected energy of the instantaneous values of coefficients of the input signal $x(n)$ [26].

The output of the adaptive filter is $y(n)$; it is calculated as

$$y(n) = w^H(n)x(n) \tag{3.8}$$

An error signal is the difference between the desired signal and the adaptive filter output, which is given as

$$e(n) = d(n) - y(n) \tag{3.9}$$

The step size can be calculated as

$$\mu(n) = \frac{\beta}{c+|x(n)|^2} \tag{3.10}$$

where,

- $\mu(n)$ is step-size at sample n
- β is the normalized step size which varies between 0 and 2.
- c is a safety factor; it is a small positive constant. It is essential because sometime $x(n)$ is very small, and then it can be difficult to calculate the weight updating equation.

The filter weights are updated for the next iteration according to the Equation 3.11,

$$w(n+1) = w(n) + \mu(n)e(n)x(n) \tag{3.11}$$

The NLMS algorithm provides better error convergence speed as compared to LMS but at the cost of higher computational complexity. This algorithm requires a greater number of computations because of the presence of a reference signal power (in this thesis context, power of the transmitted signal). The computational complexity of the LMS algorithm is O(2N+1) whereas it is O(3N+1) for the NLMS algorithm. This means that the NLMS algorithm requires N times more multiplication than the LMS algorithm. Here, N refers to the length of the coefficient vector w [26].

3.3 Background of Recursive Mean Square Algorithm

The RLS algorithm is known for its excellent performance and greater fidelity, but it is achieved at the cost of increased computational cost and complexity. This algorithm offers faster convergence and smaller error as compared to LMS for unknown system identification. These benefits make this algorithm applicable to various use cases namely echo cancellation, channel equalization, speech enhancement, interference cancellation and radar [27].

Let us assume, the input signal is $x(n)$ and $d(n)$ is the desired signal.

The output of the adaptive filter is $y(n)$, is calculated as

$$y(n) = w^H(n)x(n) \tag{3.12}$$

The error signal can be calculated according to Equation 3.13,

$$e(n) = d(n) - y(n) \tag{3.13}$$

There are two main variables which are involved in the recursion process of the RLS algorithm, namely $w(n)$ and $P(n)$ [26].

Here, $w(n)$ represents the adaptive filter coefficients, the typical initialization for this parameter is $w(0)$ =0

$P(n)$ is the inverse of the autocorrelation matrix $R_x(n)$, where

$$R_x(n) = \begin{bmatrix} r_{xx}(0) & r_{xx}(1) & \cdots & r_{xx}(N-1) \\ \vdots & \vdots & \ddots & \vdots \\ r_{xx}(N-1) & r_{xx}(N-2) & \cdots & r_{xx}(0) \end{bmatrix}$$

The approximate initialization is commonly used for this parameter which does not require matrix inversion. Thus, this parameter can be initialized as per Equation 3.14,

$$P(0) = \delta^{-1} I \tag{3.14}$$

Here, δ, this value is used to initialize the inverse of Autocorrelation at $n = 0$ and I is the identity matrix.

The gain vector, $g(n)$ can be expressed as per Equations 3.15 and 3.16,

$$g(n) = [g(0), g(1), \dots\dots\dots, g(N-1)]^T \tag{3.15}$$

$$g(n) = \frac{1}{\lambda + x'(n)P(n-1)x(n)} P(n-1)x(n) \tag{3.16}$$

The adaptive filter coefficients depend on this gain vector and can be calculated as per Equation 3.17,

$$w(n) = w(n-1) + e(n)g(n) \tag{3.17}$$

The coefficients of the auto correlation matrix can be calculated as per Equation 3.18,

$$P(n) = \frac{1}{\lambda}[P(n-1) - g(n)z^T(n)] \tag{3.18}$$

The RLS algorithm learns faster than the LMS and NLMS in a stationary environment whereas LMS performs better than RLS in a non-stationary environment. For a stationary environment, convergence behaviour of the RLS filter is the same as that of a Weiner filter whereas in case of non-stationary environment, this filter tracks the time variations. The computational complexity of the RLS algorithm is $4N^2$, which is greater than that of the LMS and NLMS algorithms.

Table 3.1 shows a comparison of three algorithms. The performance of the NLMS algorithm lies in between that of the LMS and RLS algorithms. Its computational complexity is higher than that of LMS but lower than that of RLS.

Table 3.1. Comparison of the LMS, NLMS and RLS algorithms, partly based on [27]

Parameter	**LMS Algorithm**	**NLMS Algorithm**	**RLS Algorithm**
Computational Complexity	Low O(2N+1)	More complex than LMS, O(3N+1)	More complex than both LMS and NLMS, $O(4N^2)$
Computational cost	Lower	Medium	Higher
Convergence behaviour	Slow convergence	Medium convergence	Faster convergence
Filter taps	$w(n+1) = w(n) + \mu e(n)x(n)$	$w(n+1) = w(n) + \mu(n)e(n)x(n)$	$w(n) = w(n-1) + e(n)g(n)$
Adaptation approach	Adaptation follows the gradient based approach which updates filter weights to converge to the optimum	Adaptation follows the gradient based approach which updates filter weights to converge to the optimum filter	Adaptation follows the recursive approach that finds the filter coefficients to minimize a weighted linear least squares cost function relation to the

	filter weights.	weights.	input signal.
Step size	Fixed	Adjusted at every iteration	Forgetting factor (λ) $-$ [0,1]
Older error values	Older error values play no role in the total error calculation.	Older error values play no role in the total error calculation.	All error data is considered in the total error. Using the forgetting factor, the older data can be less emphasized compared to the newer data.
Error minimization	The main objective is to minimize the current MSE.	The main objective is to minimize the current MSE.	The main objective is to minimize the total weighted squared error.

3.4 Some Experimental Results about LMS, NLMS and RLS

An experiment is conducted here to verify the convergence behaviour of LMS, NLMS and RLS algorithms. The input signal and the noise are generated using random number generators and the desired signal is produced by filtering the input signal through the FIR filter and by adding the noise. The same simulation parameters are used for all three algorithms. The number of samples are 1000, FIR filter taps are 13, step size is 0.1 and forgetting factor for RLS algorithm is 0.99.

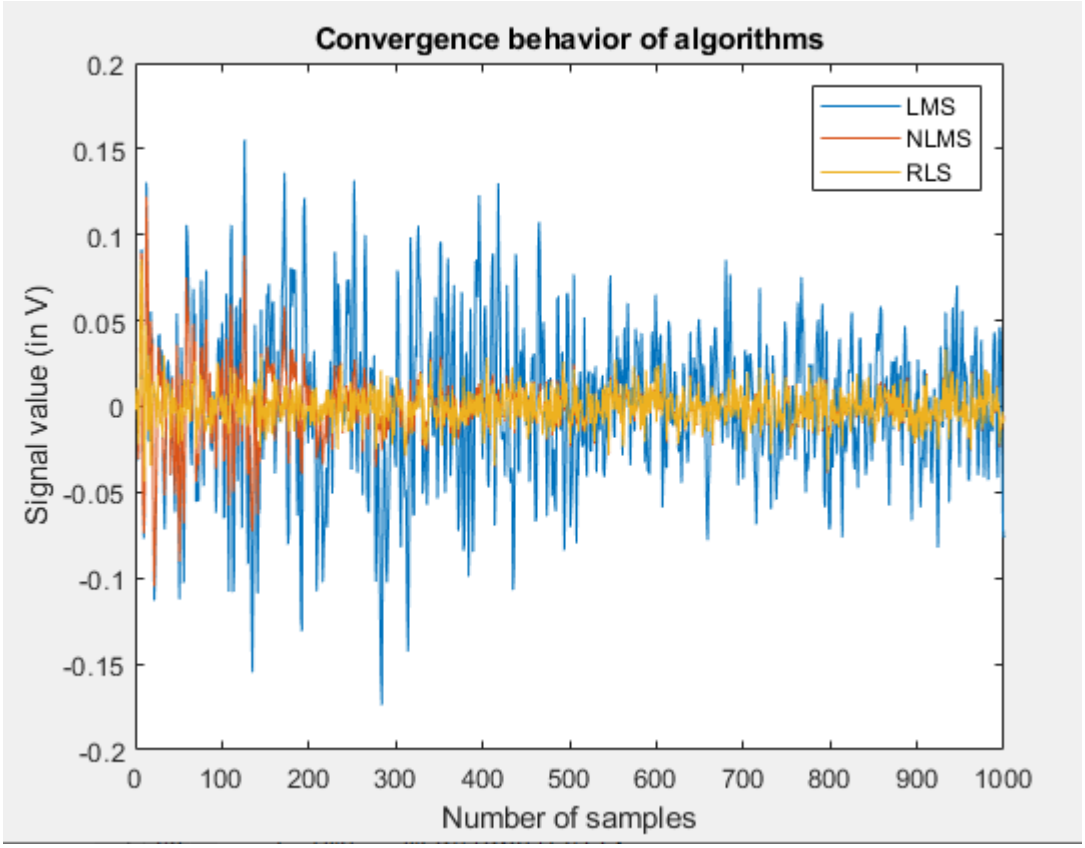

Figure 3.4. Convergence behavior of LMS, NLMS and RLS algorithms

Figure 3.4 shows that with the same simulation parameters, LMS is able to minimize the error down to 0.0349, NLMS down to 0.0127 and RLS down to 0.0088. It means that RLS performs better than LMS and NLMS as it minimized the error to the least value. It can be observed from Figure 3.4 that LMS algorithm error convergence starts after 500 samples whereas NLMS algorithm takes 150 samples to start error convergence. RLS algorithm shows faster error convergence than both LMS and NLMS and starts converging after 40 samples.

4 SI Channel Modelling

A channel is a medium that conveys the information from one or more transmitters to one or more receivers. The channel can be wired or wireless. This thesis includes the modelling of a linear wireless channel. It is well known that a wireless channel is susceptible to various transmission obstructions namely, interference, path loss, noise, shadowing, and multipath reflections. All these factors limit the data rate, range and reliability of the transmission [28]. The channel characteristics depends on the mobility of the transmitter and receiver, and the environmental conditions such as multipaths, scatters, etc. The signal strength depends on the channel characteristics.

4.1 Wireless Channel Model

In wireless communication, the three main types of channel models which govern the received signal power are named path loss, small-scale fading, and large-scale fading.

4.1.1 Path Loss Model

The path loss between a transmitter and receiver refers to the ratio of transmitted power to the received power. The amount of path loss depends on the antenna heights, link distance and environment. Path loss is directly correlated with the geographical features, so different path loss models are specified for e.g. microcell or microcells. Okumura-Hata model, Lee model, Dual slope model and Cost 231-Hata model are well known path loss models [29].

4.1.2 Large-Scale Fading

The transmission signal loss during the propagation due to reflections, absorptions, scattering and diffraction is known as shadowing or large-scale fading. E.g. in macro cell, large-scale fading can be modelled as a zero mean white Gaussian distributed variable with a standard deviation of σ_s, which is known as location variability. A

shadowing margin l_s is introduced by the location variability parameter. Probability density function of l_s [29] is defined as

$$p(l_s) = \frac{1}{\sigma_s\sqrt{2\pi}}\ exp\left[-\frac{{l_s}^2}{2{\sigma_s}^2}\right] \tag{4.1}$$

4.1.3 Small-Scale Fading

Small-scale fading model considers that the transmission signal loss during the propagation is due to multipath reflections. This model assumes that multiple delayed versions of the transmitted signal are received at the receiving end. These multiple versions of the transmitted signal combines at the receiver and the resultant signal varies widely in amplitude and phase [28]. Small-scale fading can be classified based on time dispersion or frequency dispersion based on the characteristics of the transmitted signal. Figure 4.1. shows a high-level classification of small-scale fading.

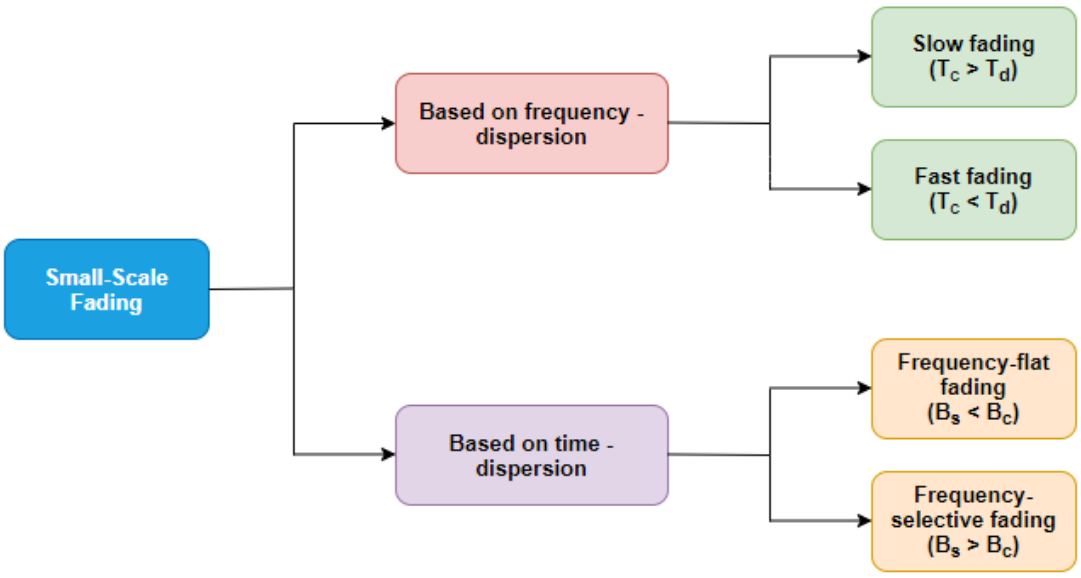

Figure 4.1. High-level classification of small-scale fading

Small-scale fading based on frequency dispersion can be classified as fast fading and slow fading. Fast fading occurs when the coherence time $(T_c)$of the channel is smaller than the symbol period (T_d). On the flip side, slow fading occurs when T_c is greater

than T_d. Moreover, the coherence time is the time duration over which the channel is considered to be invariant [29].

Small-scale fading based on time dispersion can be classified as frequency-flat fading and frequency-selective fading. Flat fading or narrow-band fading is applicable when the signal bandwidth (B_s) is less than the coherence bandwidth (B_c) of the channel. Coherence bandwidth is the range of frequencies over which the channel passes all the spectral components with approximately equal gain and linear phase. Frequency-selective fading or wide-band fading is applicable when the signal bandwidth (B_s) is greater than the coherence bandwidth (B_c) of the channel [29]. This fading affects the different frequency components of the signal in different manner. Wide-band signals experiences inter-symbol interference (ISI), so these requires equalizers for compensation whereas no equalizer is required for narrow-band signals.

A time-varying channel with frequency-selective or wide-band fading can be modelled as a linear filter with time varying tap coefficients [29], where the number of taps represents different multipaths. A tapped delay line channel model is shown in Figure 4.2. Here, let us assume N_m is the number of paths and the delay of each path is denoted by τ_n. The tap gain of each tap is denoted as $h_n(t)$ whereas the input and output signal are denoted as $u(t)$ and $y(t)$. The output of tapped delay line channel model is as follows,

$$y(t) = \sum_{n=0}^{N_m} h_n(t)u(t-\tau_n) \tag{4.2}$$

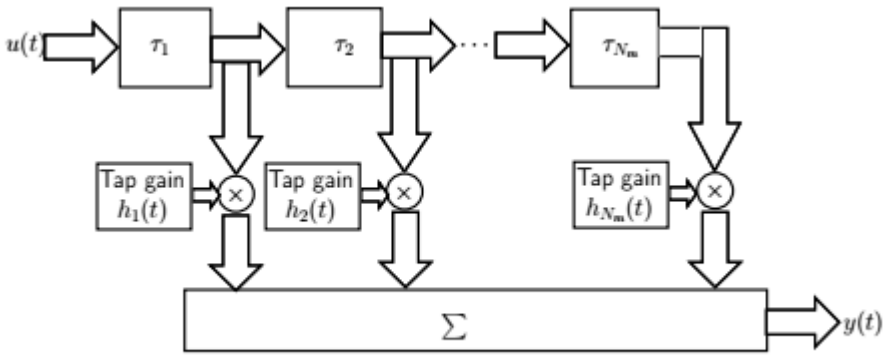

Figure 4.2. Tapped delay line channel model [29]

4.2 SI Channel Modelling

The amplitude of a multipath channel with small-scale fading effect can be modelled with the probability distribution function such as Nakagami-m, Lognormal or Weibull, but this thesis uses only on Rician and Rayleigh distribution (in this context of this thesis, SI channel is modelled as Rician channel whereas Rayleigh channel is modelled for the desired signal). For this thesis, the Rician fading channel is an appropriate choice because the transmitting and receiving antenna are closely located in the transceiver, this channel is quite useful to implement as a SI coupling channel.

4.2.1 Rayleigh Fading Channel

Rayleigh fading is a statistical model for modelling a wireless channel. The magnitude of the signal varies randomly or fade, according to a Rayleigh distribution. A signal going through Rayleigh fading undergoes deep fades, so, this model is applicable for different practical scenarios such as radio signal propagation in urban environments and, tropospheric and ionospheric signal propagation [30]. This fading does not have any line of sight path (LOS) or specular component between the transmitter and receiver.

The fading amplitude r_i at ith time instant can be expressed as [30]

$$r_i = \sqrt{(x_i + \beta)^2 + {y_i}^2} \tag{4.3}$$

where x_i and y_i are samples of zero-mean stationary Gaussian random processes each with variance σ^2 and β is the amplitude of the specular component.

The probability density function (PDF) of Rayleigh distribution can be expressed as [30],

$$f_{rayleigh}(r > 0) = \frac{r}{\sigma^2} e^{-r2/2\sigma^2} \tag{4.4}$$

4.2.2 Rician Fading Channel

Rician fading is also a statistical model for modelling wireless channel and magnitude of the signal varies randomly, according to a Rice distribution. The fading is Rice if the multiple reflective paths are large and strong dominant LOS component. This multipath fading model consist of one LOS path whereas others are non-line-of-sight (NLOS).

The probability density function (PDF) of Rice distribution can be expressed as [30]

$$f_{rice}(r > 0) = \frac{r}{\sigma^2} e^{(-r^2+\beta^2)/2\sigma^2} I(r\beta/\sigma^2) \quad (4.5)$$

Rician K-factor express the ratio of the specular to diffuse energy components or it determines how strong the LOS component with respect to other NLOS component. Mathematically, Rician K-factor can be represented as [30],

$$K = \beta^2/2\sigma^2 \quad (4.6)$$

The special cases of Rician fading channel are associated with this K-factor. When $K = \infty$, the channel behaves like Gaussian channel with strong LOS path whereas, for $K = 0$, the channel follows Rayleigh distribution with no LOS path.

4.2.3 Some Experimental Results related to Channel Modelling

In this thesis, some experiments are performed in MATLAB to validate the theoretical concepts of the channel modelling. Let us assume that channel is linear and is not affected by the non-linearities such as PA non-linearities and IQ imbalance. For this thesis, the Rician fading channel is an appropriate choice because the transmitting and receiving antenna are closely located in the transceiver, this channel is quite useful to implement as a SI coupling channel. In other words, the received signal is highly correlated with the transmitted signal when passed through the Rician channel.
The simulation parameters which are used to model the Rician channel are summarized in Table 4.1.

Table 4.1. Simulation parameters for modelling of Rician channel

Parameter	Value
Sample Rate	500 kHz (Frequency Selective Fading)
Path delays	[0 3 6] e-6
Average path gains	[0 -5 -10]
Maximum Doppler Shift	80 Hz
K factor	10

The MATLAB object function which is used to simulate the Rician channel is given as

```
ricChan = comm. Rician Channel (...
    'Sample Rate’,          sampleRate500kHz, ...
    'Path Delays’,           delay Vector, ...
    'Average Path Gains',        gain Vector, ...
    'Maximum Doppler Shift’,     max Doppler Shift, ....
    'K Factor', K Factor,..
    'Path Gains Output Port’,   true);
```

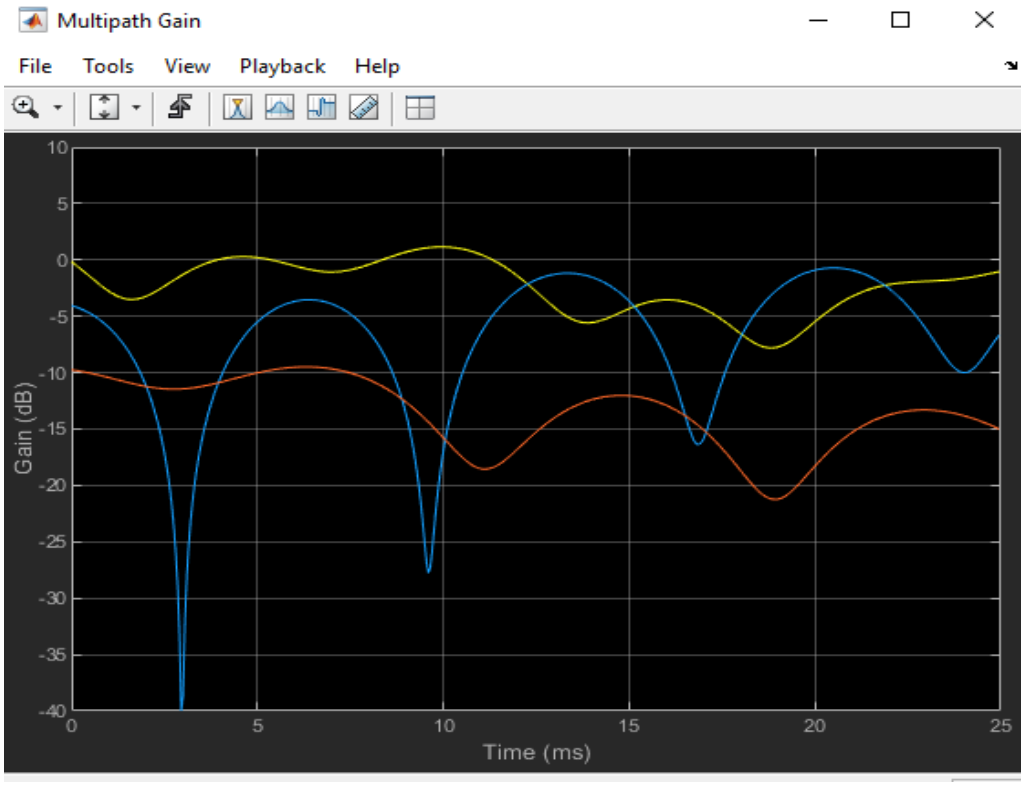

Figure 4.3. Multipath Gain of three different paths of Rician channel, the yellow curve corresponds to the first path (LOS), and blue and red curves correspond to the second and third paths (NLOS)

Figure 4.3. depicts the multipath gain of three different path of Rician channel. The first path of the Rician channel is always in LOS and experience little fading, which can be observed from the above figure 4.3 (yellow curve). Another two paths are NLOS and experience more fading (blue and red curves).

5 Experimental Setup for the - Pseudo Real-Time Implementation of FD System

In Chapter 5, a pseudo real-time implementation of FD system is presented. Firstly, for generating the signals, the GNU Radio environment is used to design a flowgraph for real time transceiver using two Lime SDRs; the transmitted and received signals are stored in file sinks. Secondly, the digital SIC is performed in the MATLAB environment in offline mode, hence the name pseudo real-time. The source code for the linear digital SIC using LMS algorithm is presented in Appendix 2.

5.1 Experimental Setup

The experimental setup to implement the pseudo real-time implementation of FD system includes both hardware and software. The description of hardware and software is as follows:

- **Hardware**
  - Laptops/PCs x 2
  - Lime SDR-USB boards with USB Type A plug x 2
  - 1 m long RF cables x 2
  - Telescopic Antennas SMA (ANT500) x 3
  - USB cables x 2
- **Software**
  - GNU Radio Companion 3.7.13.5
  - MATLAB R2019a – academic use

Figure 5.1 shows the experimental setup for implementation of the pseudo real-time FD system. The experimental setup is divided into a near-end signal and a far-end signal. For the near-end signal, a Lime SDR-USB is connected to a laptop/PC using a USB cable. In the first experiment, a 1 m long RF cable is used to connect the transmitter port and the receiver port of the same SDR board (antennas are used in second set of experiments). This RF cable acts as a channel through which the transmitted channel travels and is received as the SI signal at the receiver port. This near-end signal is also called SI signal.

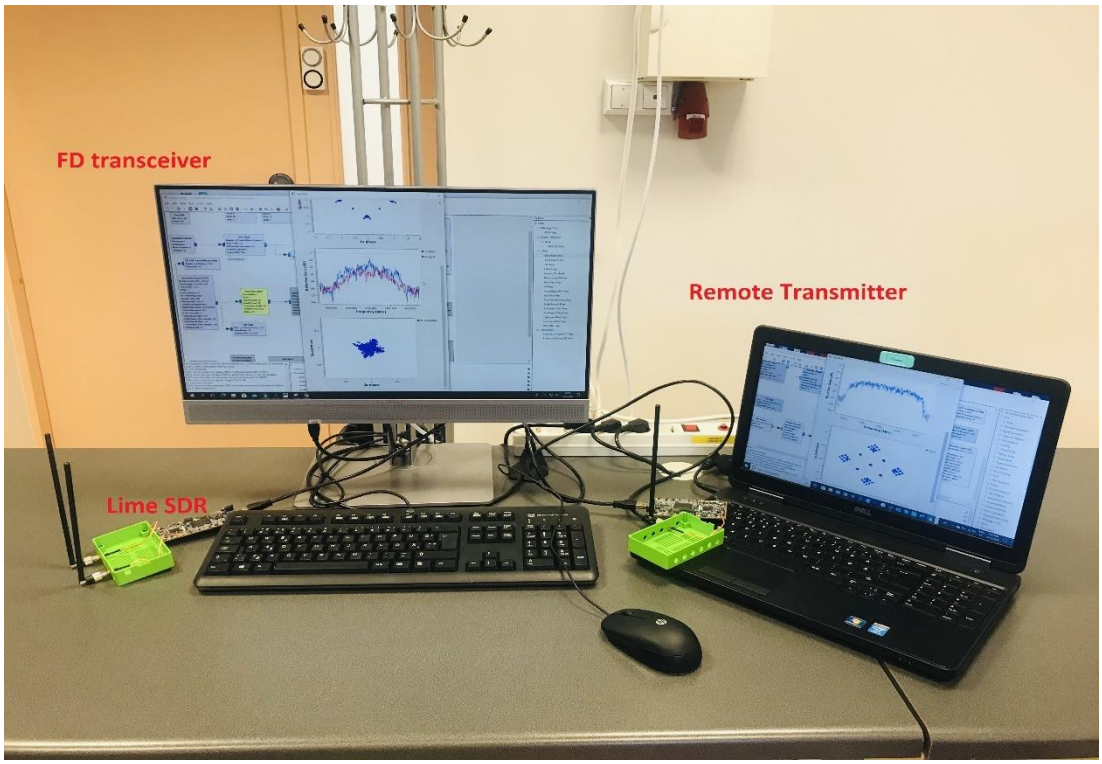

Figure 5.1. Experimental setup for the pseudo real-time implementation of FD system, here shown with the antennas, installed in one of Thomas Johaan Seebeck Department of Electronics'labs

For the far-end signal, another Lime SDR-USB is connected to second laptop/PC using a USB cable. Again, a 1 m long RF cable is used to connect the transmitter port of the second Lime SDR and the receiver port of the first Lime SDR board (the cable is also replaced by antennas in a second set of experiments). This RF cable acts as a channel

through which this additional transmitted channel travels and is received as the desired signal at the receiver port. This near-end signal is also called remote/desired signal.

Moreover, GNU Radio Companion and MATLAB are installed on both computers to design the flowgraph and coding, respectively.

5.2 Lime SDR-USB

Lime SDR is an open source SDR that supports wide range of wireless communication standards; for example, it is capable to transmit and receive UMTS, LoRa, LTE, GSM, Bluetooth, RFID, etc [31]. It consists of the required RF front-end as well as a digital backend to receive and transmit the baseband signal from the SDR board over the USB to a connected host device (typically a PC). The hardware architecture of the Lime SDR is shown in Figure 5.2.

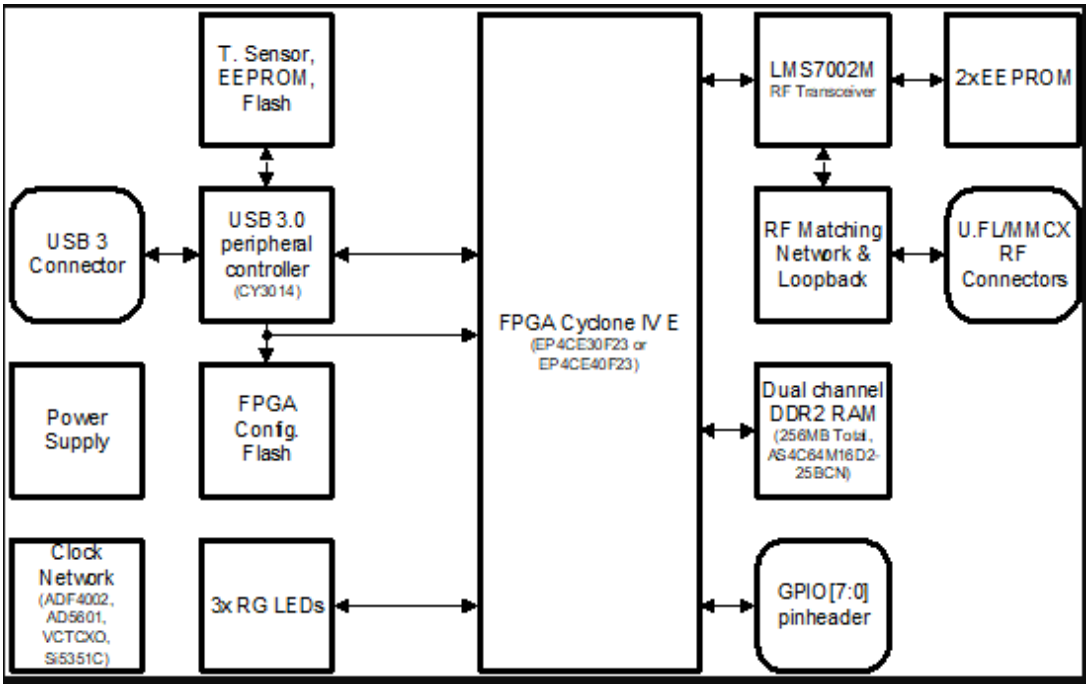

Figure 5.2. Lime SDR-USB development board block diagram [31]

Altera (now Intel) Cyclone IV FPGA is the heart of the Lime SDR-USB board and its main function is to transfer digital data between the PC and the Lime LMS7002 RF

transceiver through a USB3.0 connector. The USB 3.0 controller and peripherals are located on left hand side of the block diagram.

- **Key features and specifications**

Table 5.1 summarizes the main features and specifications of the Lime SDR-USB board.

Table 5.1. Key features and specifications of Lime SDR-USB [31]

S.No	Feature	Description
1.	RF Transceiver	Lime Microsystem LMS7002M MIMO field - programmable RF (FPRF)
2.	Frequency Range	100 kHz – 3.8 GHz
3.	RF Bandwidth	61.44 MHz
4.	Sample Rate	61.44 MSPS
5.	RF frontends	2 Rx/Tx
6.	Power Output	Up to 10 dBm
7.	Multiplexing	2x2 MIMO

- **Lime SDR-USB RF Ports**

The Lime SDR-USB consists of two Rx and two Tx channels where each Tx channel offers two different output ports and each Rx channel offers three different input ports. These channels are identical and can be used for Multiple Input-Multiple Output (MIMO) setups if required. Table 5.2 shows the description of Lime SDR-USB RF ports. In this thesis context, the target RF centre frequency is 2.4 GHz. Therefore, the selected receiver RF port is RX1_H (Channel 1 RX) and the transmitter RF port is TX1_1 (Channel 1 TX). Channel 1 or A is used for transmission and reception of the signals. Channel 1 + channel 2 can be used for MIMO set up.

Table 5.2. Lime SDR-USB RF Ports [31]

S.No	Label	Description
1.	RX1_H	Channel 1 RX: frequencies above 1.5 GHz
2.	RX2_H	Channel 2 RX: frequencies above 1.5 GHz
3.	RX1_L	Channel 1 RX: frequencies above 1.5 GHz
4.	RX2_L	Channel 2 RX: frequencies above 1.5 GHz
5.	RX1_W	Channel 1 RX: wideband
6.	RX2_W	Channel 2 RX: wideband
7.	TX1_1	Channel 1 TX: primary (all frequencies)
8.	TX2_1	Channel 2 TX: primary (all frequencies)
9.	TX1_2	Channel 1 TX: secondary (all frequencies)
10.	TX2_2	Channel 2 TX: secondary (all frequencies)

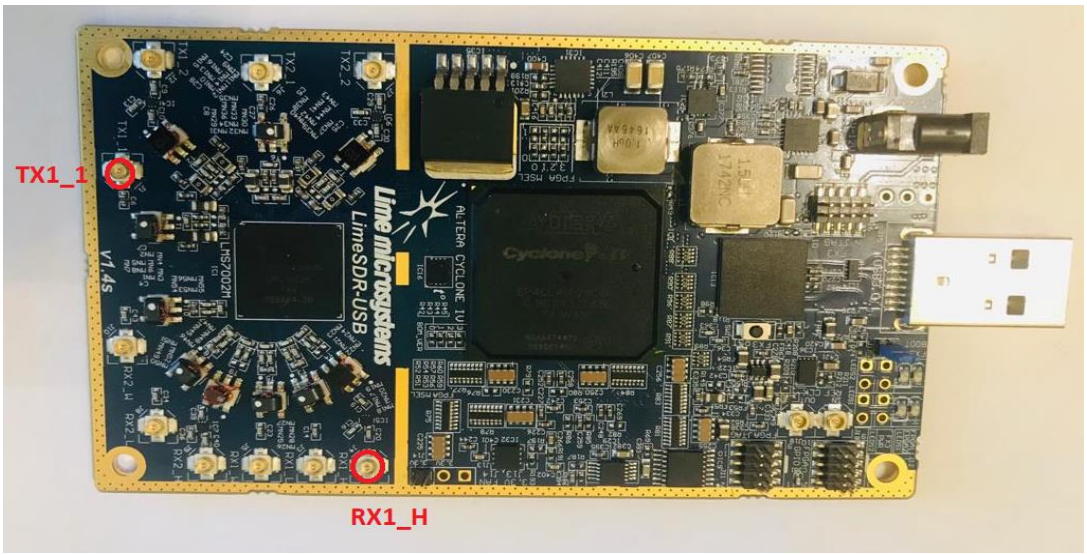

Figure 5.3. Photograph of the Lime-SDR USB board, TX/RX RF ports (TX1_1, RX1_H) selected for the real-time implementation are highlighted

The connections of TX/RX RF ports are shown in Figure 5.3 which are used for real-time implementation of FD system in this thesis.

5.3 Simulation Model

GNU Radio Companion is a graphical tool for creating signal flow graphs for SDR applications; in this this thesis, it is mostly used to design the simulation model/flow graph for real-time FD system.

The flowgraph is divided into two sections, namely transceiver and remote transmitter. Here, the transceiver acts as a FD system, it has the capability to transmit and receive simultaneously on the same frequency. The receiver receives the desired signal from the remote transmitter as well as the SI signal from its own transmitter. This conceptual idea is used to design the flow graph of the FD system in this thesis.

In Figure 5.4, a flow graph of the developed FD system is presented. The upper part of the flow graph shows the FD node (transceiver) whereas the lower part is the remote transmitter which transmits the desired signal.

The SI signal is created using a random stream of bits and then modulated onto a complex constellation. A Constellation Modulator block is used to create the complex constellation whereas, a constellation object is created for the settings to control the QPSK modulated transmitted signal. Thus, a QPSK signal is transmitted as the SI signal. A basic Channel Model block is used for the modelling of the SI channel. This block allows us to set the values of additive noise, frequency offset and timing offset. In this particular case, the value of additive noise is 100 µV and the frequency offset is 0. Here, the noise power is set by adjusting the noise voltage value of the channel model and the voltage is specified instead of power because the bandwidth of the signal is unknown in order to the power properly. Initially, the adjusted value of additive noise voltage is small and frequency offset is set to 0 and then further increases to analyse their effect on the transmitted constellation. Eventually, the SI signal travels through the channel and is received at the receiving end. There is one adder block on the receiving port which adds the SI signal and the desired signal.

The desired signal is also a QPSK modulated signal, but it travels through a Rician fading channel and the output signal is stored in a virtual sink. Then, this faded desired

signal is read by the virtual source and added to the add block at the receiving port. The recovery of the received signal starts with timing recovery. The Polyphase Clock Sync block is used for timing recovery of the incoming signal. It seeks to find the best time to sample the received signals which helps to maximize the SNR of each samples and to reduce the effects of interference. This block is setup with 32 filters to find the desired timing value of the samples. It is given in [32] 32 filters can give a maximum inter-symbol interference (ISI) noise factor that is less than the quantization noise of a 16-bit value. More filters can be used if more than 16 bits of precision is required.

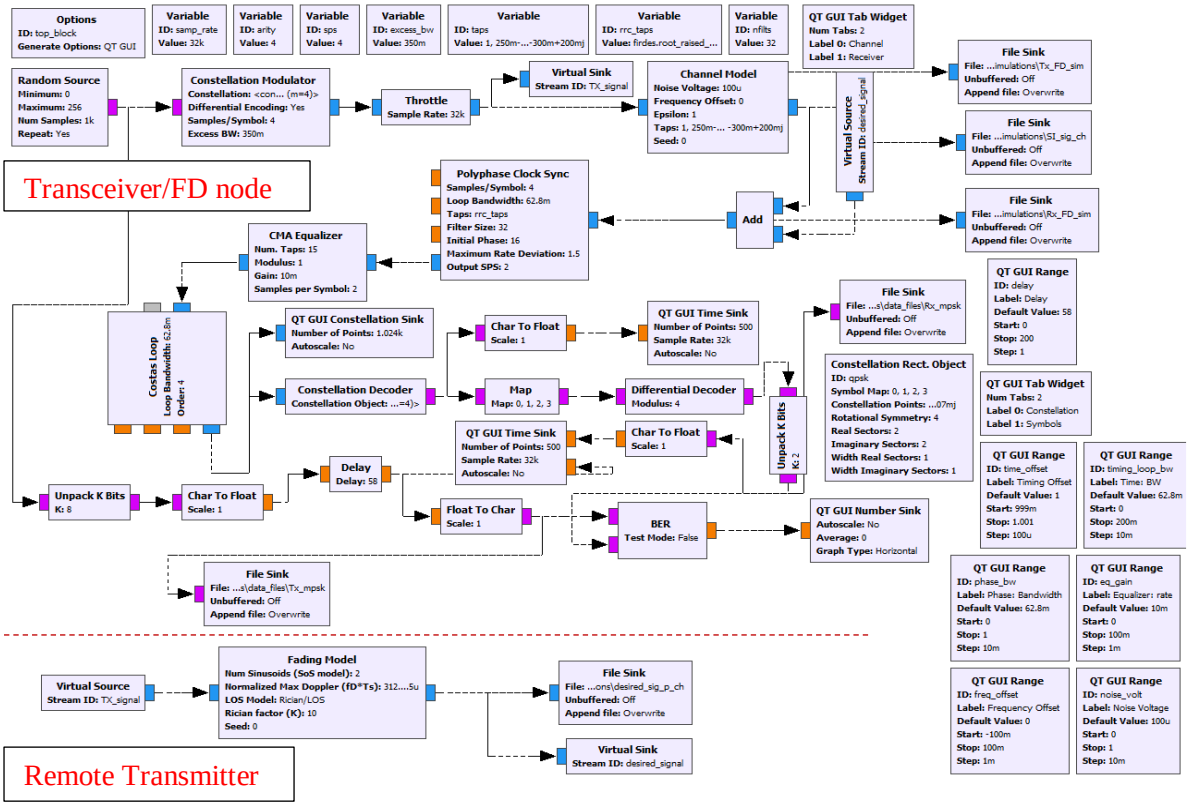

Figure 5.4. Simulation model /Flow graph of FD system

Next stage is to undo the distortion (multipath effects) that is caused by the channel. A Constant Modulus Algorithm (CMA) equalizer is used to invert the channel effect. This equalizer is suitable for an MPSK signal as they have points only on the unit circle. The next task is to correct the frequency and phase offset.

The Costas Loop block is used to synchronize the QPSK signal and lock the constellation with the noise. Now, the Constellation Decoder block decodes the symbols from 0 to 3 as per the alphabet size (4 in QPSK case) and then the Differential Decoder block translate the differential coded symbols back to their original symbols. At this point, the original symbols are recovered, and the Unpack Bits block is used to unpack those 2 bits per symbol into bits. Finally, the original bit stream of data is available at this point.

A BER block is inserted in the flow graph to find the error rate between the transmitted and the received bits. But, the most important point is to synchronize the transmitted signal and the received signal because the receiver chain has many blocks and filters that delay the received signal. So, a Delay block is used to compensate the delay between the two signals. Finally, synchronized bits are used to calculate the bit error rate.

In this flow graph, the receiver chain is simulated to understand the different steps to design a receiver and to visualize the effect of SI signal in FD mode, keeping in mind that the figure of merit in the context of this thesis is amount of digital cancellation and minimization of mean square error (MSE).

5.4 Flow Graph for Real-Time Implementation of FD System

The developed design of the flow graph for real-time implementation is approximately the same as the simulation model, excepts for some blocks, as explained in what follows.

In Figure 5.5, the hardware blocks Lime Suite Sink (TX) is used to transmit the signals and Lime Suite Source (RX) is used to receive the physical signals, which are shown within the red blocks. The channel models are replaced with the RF cables/antennas and the Throttle block (used to control average rate) is also removed because now actual hardware is used. Moreover, one new block Multiply Const is inserted in between the Constellation Modulator and Lime Suite Sink (TX) to control the amplitude of the signal fed to the hardware TX.

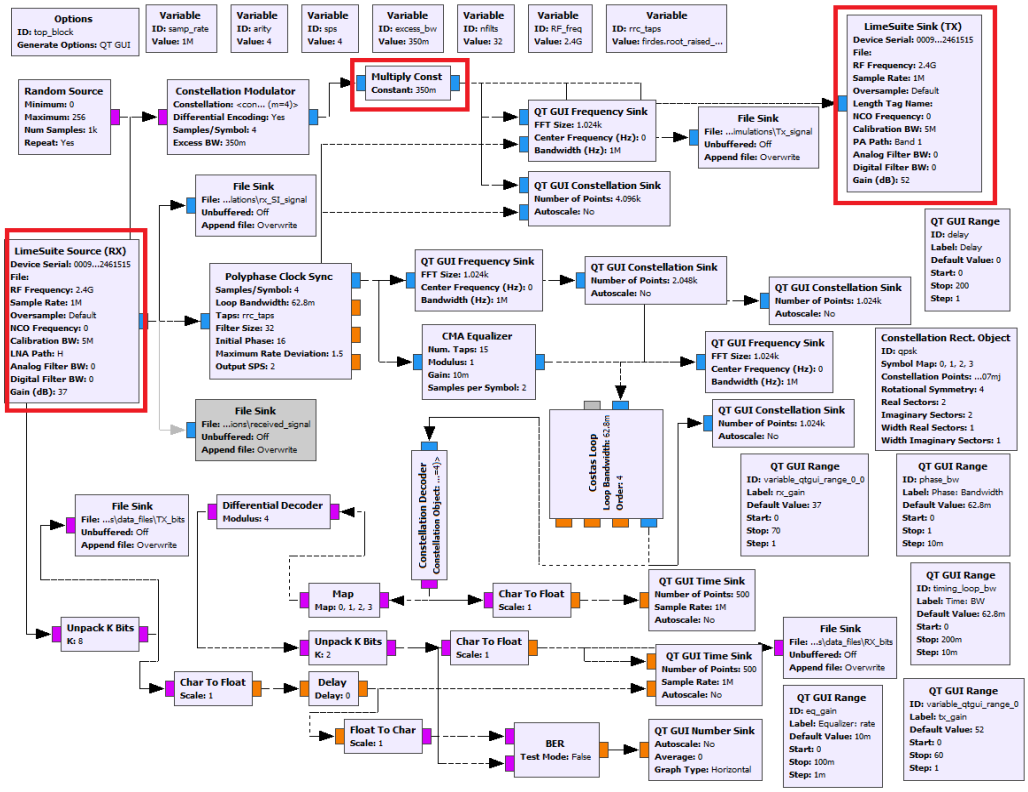

Figure 5.5. Flow graph for pseudo real-time implementation of FD system

The transmitted and received signals are stored in the GRC environment and later used in MATLAB to implement digital SIC in offline mode.

5.5 Workflow of Pseudo Real-Time Implementation of FD System

The workflow of implementation of pseudo real-time FD system comprises of the following steps:

- Generate SI signal and desired signal using flow graph design in GRC environment.
- Transmit both the signals through the channel model in the case of simulation/ through the RF cables/ antennas in case of real-time implementation.
- Store the transmitted signal and received signal (combination of SI signal and desired signal) in file sink blocks of GNU Radio Companion.

- Read these .bin files in MATLAB and cross correlate the transmitted and received signal to synchronize the files;

- Implement the LMS adaptive algorithm for digital SI cancellation. First, LMS algorithm reconstructs the SI signal from the transmitted signal and then subtracts the received signal and reconstructed SI signal to find the amount of digital cancellation;

- All the above steps are repeated for the three different cases: implementation with simulation, transmission/reception with RF cables, transmission/reception with antennas.

6 Simulation and Implementation Results and Analysis

This chapter is divided into two sections. The first section consists of the waveform simulation results of linear digital SIC for FD system using the different adaptive filtering algorithms LMS, NLMS and RLS presented in Chapter 3. The source code is presented in Appendix 1.

In the second section, the pseudo real-time FD system is implemented using Lime SDRs with GNU Radio Companion (GRC) and MATLAB. The GNU Radio with Lime SDRs are used to transmit and receive real-time signals and then stored in file sink. The digital SI cancellation is performed in MATLAB using the LMS algorithm.

Moreover, the results for the above setups are presented and analysed.

6.1 Linear Digital SIC for FD System

A linear digital SIC has been performed for an FD system using three different algorithms. For this simulation, the nonlinear effects of PA and IQ imbalance are not considered. The digital SI cancellation technique using LMS algorithm is presented in Figure 3.1 (Chapter 3). Initially, QPSK modulated signals are generated to create both the known transmitted signal and the unknown desired signal. The SI signal is generated when the transmitted signal passes through the Rician channel (the SI channel modelling is described in Section 4.2). The linear multipath SI channel is modelled as a Rician fading channel and the desired signal channel as a Rayleigh fading channel. The received signal at the receiver antenna is the combination of the SI signal, desired signal, and noise. The next step involves the estimation of the SI channel and here, it is estimated using the three different filtering algorithms (LMS, NLMS and RLS). SI cancellation is performed after the subtraction of the received signal and estimated SI signal; the remaining signal is called residual signal.

The simulation parameters are summarized in Table 6.1. To evaluate the performance of these three different algorithms for a FD system; the figure of merits for this FD system are MSE and amount of SI cancellation.

Table 6.1. Simulation parameters for digital SIC

S. No	**Parameter**	**Value**
1.	Number of samples (N)	1000
2.	Number of trails	1000
3.	Constellation	QPSK
4.	SI channel length	5
5.	Signal to Residual Interference ratio (SIR)	-20 dB
6.	Signal to Noise ratio (SNR)	20 dB
7.	Number of taps of adaptive filter	5
8.	Step size of LMS algorithm	0.002/varied [0,2]
9.	Step size of NLMS algorithm	0.00012
10.	Forgetting factor of RLS algorithm	0.9999

Figure 6.1 depicts the absolute values of the impulse responses of the SI channel and estimated channels using LMS, NLMS and RLS algorithms. In the code, the Rayleigh fading channel with channel response (H) is modelled for the desired signal; please refer to Appendix 1. H is the product of an L x 2 matrix and a 2x1 matrix [1; j]. That is, H is of the form $\frac{1}{\sqrt{2}} * (X + jY)$ where j is the square root of unity and X and Y are zero mean

unit variance gaussian distribution. The factor $\frac{1}{\sqrt{2}}$ is used to make the power of the resultant signal unity (normalization factor). This is done to ensure that the fading does not accidentally amplify the message. The resulting distribution is called a complex gaussian distribution. The absolute value of the complex gaussian distribution is Rayleigh distributed.

Next, the SI channel is modelled using Rician fading distribution. In the source code, SIR_pre = -20 means the SI channel is 20 dB power boosted w.r.t the normal channel H. That is, the SI channel has a power 20 dB higher desired signal channel. Therefore, the coefficients of Rician fading channel are multiplied with $10^{-(\frac{SIR_{pre}}{10}/2)}$. Here the unit variance complex Gaussian channel is multiplied with an amplitude $10^{-(\frac{SIR_{pre}}{10}/2)}$.

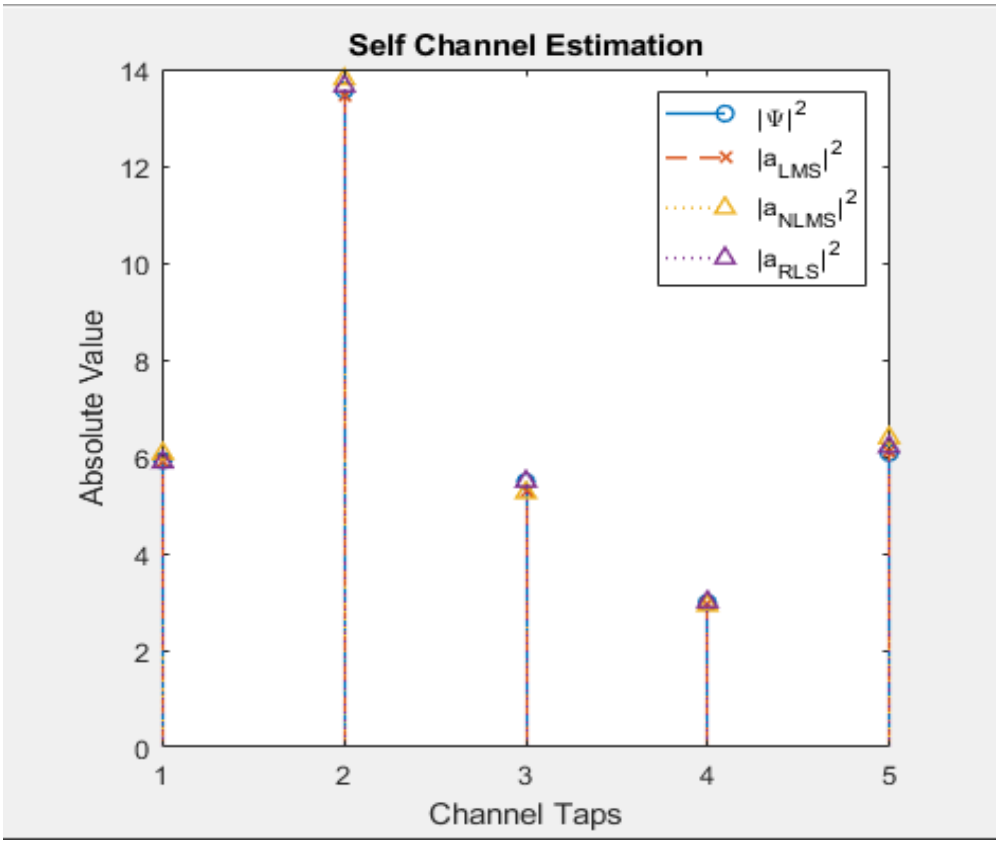

Figure 6.1. Absolute values of impulse responses of SI channel and estimated channels using LMS,NLMS and RLS algorithms

For the channel estimation, the number of taps of adaptive filters (LMS, NLMS and RLS) is 5. Three different functions named DF_LMS(), DF_NLMS(), and DF_RLS() are created to find the coefficients of the estimated channel using the above defined algorithms. It is known that updating of the weights of the adaptive filters is an iterative process and the updated weight depends on the present weight, error term, step size and input signal. For the LMS algorithm, the step size is 0.002 which is fixed for every iteration whereas the step size for the NLMS algorithm can be adjusted in every iteration.

In Figure 6.1, the marker symbol in blue colour depicts the absolute values of the channel response of SI channel, whereas the red, yellow and purple markers show the absolute values of channel estimation using LMS, NLMS and RLS algorithms, respectively. It can be observed from Figure 6.1 that the purple (RLS) marker approximately overlap the values of the SI channel, whereas the yellow and red markers slightly vary. Therefore, the performance of the RLS algorithm is better than that of the LMS and NLMS for channel estimation whereas LMS has the lowest performance when estimating the SI channel. These simulation results are in line with the theory presented in Chapter 3.

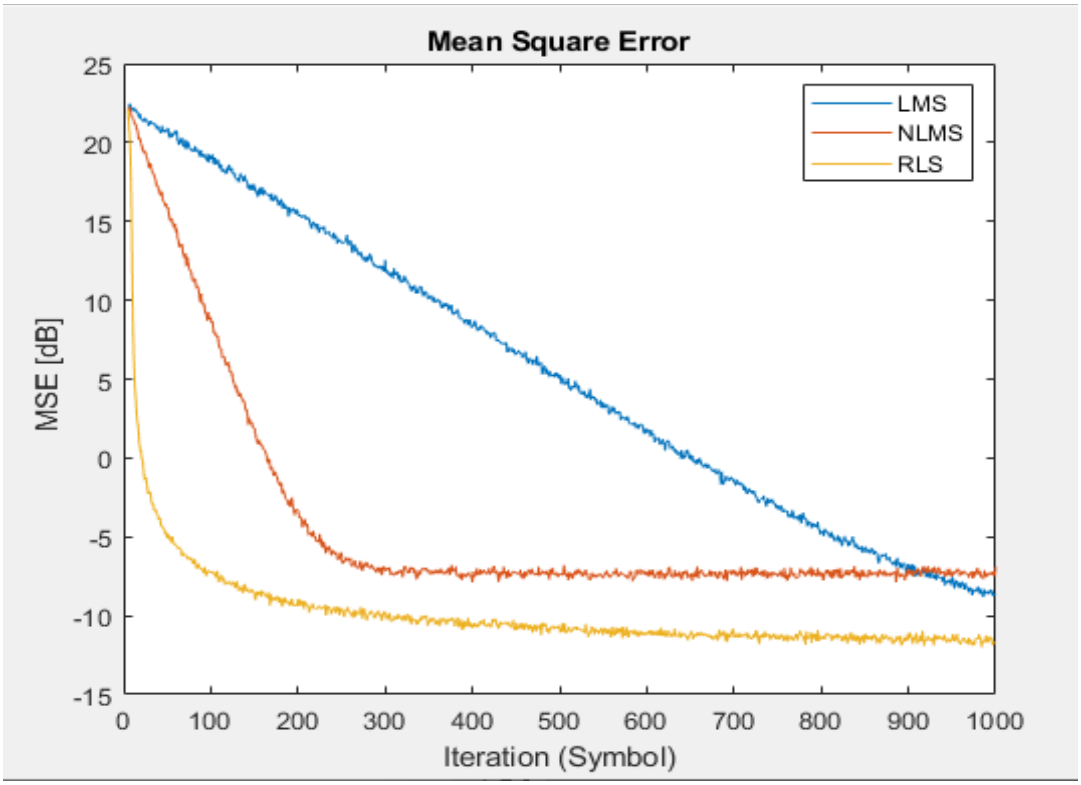

Figure 6.2. Average MSE of LMS, NLMS and RLS algorithms

Figure 6.2 shows the average MSE which is plotted using the LMS, NLMS and RLS algorithms. It can be seen from the figure that the LMS algorithm takes almost 900 samples to converge whereas NLMS takes approximately 210 samples and only around 40 samples are taken by the RLS algorithm. Therefore, the RLS algorithm shows faster error convergence than both the LMS and NLMS algorithms; the slowest error convergence is shown by the LMS algorithm. These simulation results are also in line with the theory and initial simulation results presented in Chapter 3. The algorithms of Figure 3.4 follow the same pattern of error convergence as followed by the algorithms in Figure 6.2.

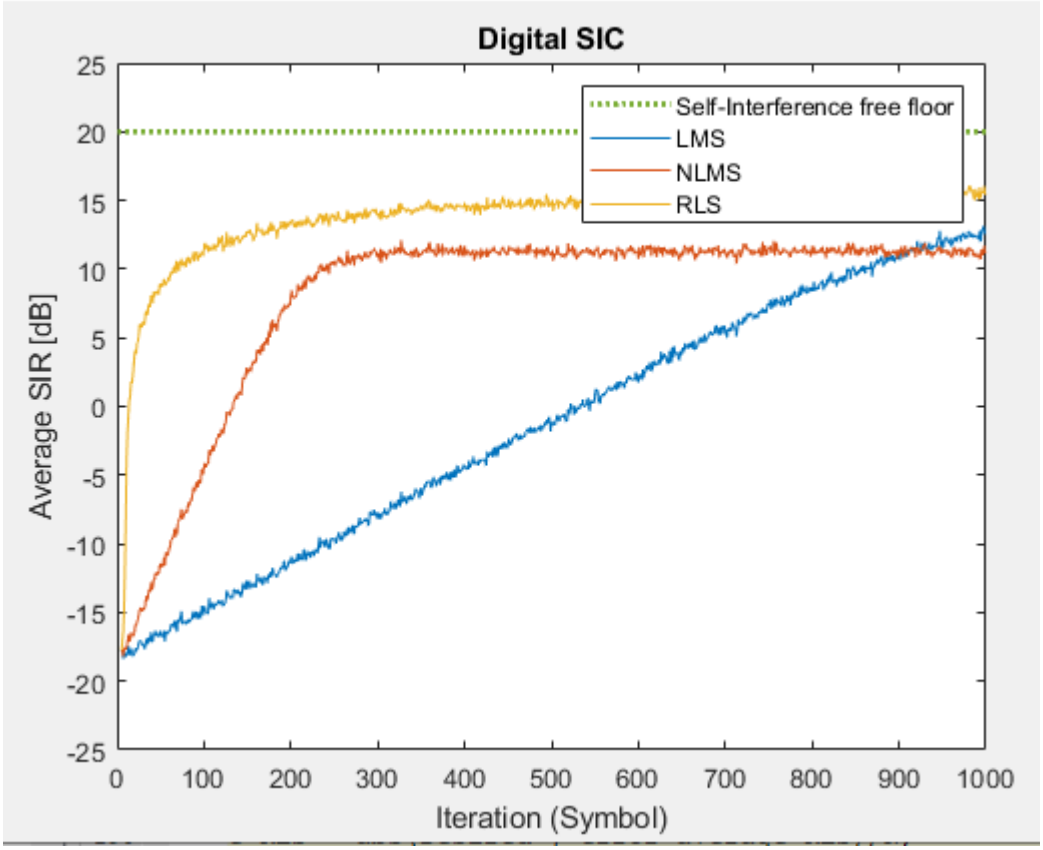

Figure 6.3. Comparison of average SIR level for LMS, NLMS and RLS algorithms

Figure 6.3 shows the comparison of the average SIR level or digital canceller output for the LMS, NLMS and RLS algorithms. The power of self-interference floor is 20 dB and the defined signal to residual interference ratio is -20 dB. It can be analyzed from the figure that the SIR level increases with the number of iterations. With the use of LMS algorithm, the SIR level increases up to 10 dB, but it takes 900 samples or iterations to

reach that point, whereas with the NLMS algorithm, this point is achieved with only 210 samples/iterations. Moreover, the RLS algorithm takes only 10 samples to reach 10 dB SIR level. The maximum achieved SIR level is approximately 15 dB by using RLS algorithm which is very close of self-interference free floor.

In other words, it is possible to achieve 30 dB of SI cancellation using the LMS algorithm but at the cost of more iterations/samples, whereas the approximately same amount of SI cancellation is achieved by NLMS with a smaller number of samples/iterations. Moreover, 35 dB of SI cancellation is achieved by the RLS algorithm and it takes a much smaller number of samples/iterations than the LMS and NLMS. The simulation results follow the theoretical aspects which are presented in Chapter 3.

In a nutshell, by analyzing the simulation results, one can make the statement that the performance of the RLS algorithm stands out from the simulated three algorithms. However, although the performance of RLS is better than the NLMS and LMS algorithms, the main drawback of the RLS algorithm is its higher computational complexity and implementation cost. In [33] a comparison of design and implementation of LMS and RLS filters is shown for real-time, implemented using VHDL design and Xilinx synthesis tools. For real-time implementation, researchers prefer the LMS algorithm over NLMS and RLS due to its computational simplicity, ease of implementation, unbiased convergence and lower implementation cost. Therefore, LMS algorithm is used in the rest of the thesis for pseudo real-time implementation.

6.2 Pseudo Real-Time Implementation of FD System

For the result analysis, Section 6.2 is divided into three cases. The first case shows the results of the simulation model of a FD system. The second case reflects the results of the pseudo real-time FD system when RF cables are used for transmission and reception whereas the results of the pseudo real-time FD system over the air (with antennas) are presented by the third case.

Case 1: Simulation model of FD system

The flow graph of the FD system is already defined in section 5.3; this section shows key results. The main simulation parameters for FD system are presented in Table 6.2. The experiment is performed by considering two cases: receives only transmitted signal aka SI signal and another is to receive the SI signal and desired signal.

Table 6.2. Key simulation parameters of flow graph of FD system

S.No	Block	Parameter	Value
1.	Constellation Modulator	Constellation Samples per symbol	QPSK 4
2.	Throttle	Sampling rate	32 kSPS
3.	Channel Model	Taps	[1.0, 0.25-0.25j, 0.50 + 0.10j, -0.3 + 0.2j]
4.	Polyphase Clock Sync	Samples per symbol Filter size Output samples per symbol	4 32 2
5.	CMA Equalizer	Number of Taps	15
6.	Fading Model (Rician)	Rician factor	4

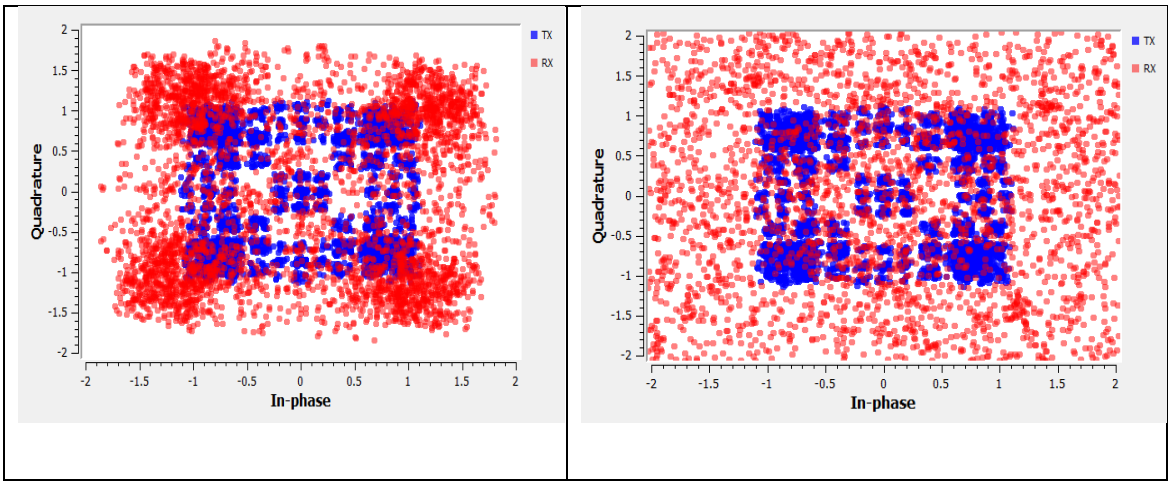

Figure 6.4. Constellation diagrams of SI signal alone (left) and received signal (SI signal and desired signal, right)

Figure 6.4 depicts the constellation diagrams of the received SI signal alone (left) and the combination of the received SI signal and the received desired signal (right). It can be observed that the constellation points on the right-hand side of the plot are more scattered due to combination of the SI signal and the desired signal. However, these constellation points can be improved by using some particular blocks, namely Polyphase Clock Sync, CMA Equalizer and Costas Loop in the receiver chain which are described in Section 5.3.

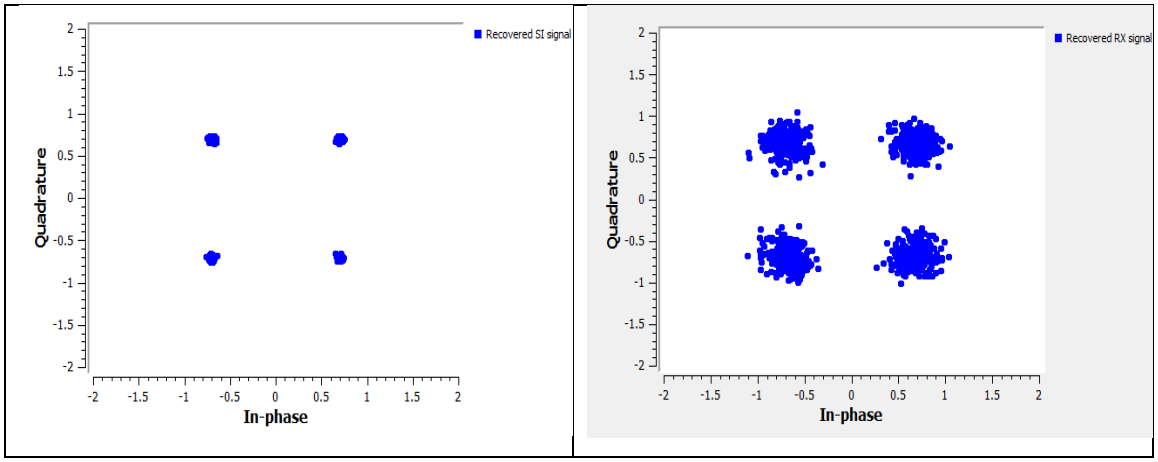

Figure 6.5. Constellation diagrams of the recovered SI signal (left) and the received signal (SI signal and desired signal, right)

Figure 6.5 shows the constellation diagrams of the recovered signals by the receiver chain. It is clearly visible from the constellation diagrams that the receiver chain can converge the constellation points much closer to the ideal points. The measured BER of recovered SI signal is $10^{-4.83}$ whereas for the recovered RX signal it is $10^{-2.34}$, which is almost half of the former BER. So, it can be concluded that the BER error increases in case of combination of the SI signal and the desired signal due to interference. The results also show that the recovery blocks help in improving the performance significantly. The main purpose to present these results in this section is to elaborate the concept of FD system when it receives two signals at the same time. However, the main aim is to find out the amount of SI cancellation achieved in FD system, as discussed in what follows.

As mentioned earlier, the digital SIC is performed in MATLAB. So, to implement digital SIC the transmitted signal and the received signal are saved in files in the GRC environment and then read in MATLAB. The LMS algorithm takes the input samples from the transmitted signal and then reconstruct the SI signal and finally calculates the amount of SI cancellation. The main simulation parameters of digital SIC are shown in Table 6.3.

Table 6.3. Simulation parameter of digital SIC

S.No	Parameter	Value
1.	Number of samples	500 k
2.	Step size	0.067
3.	Estimation filter taps	6

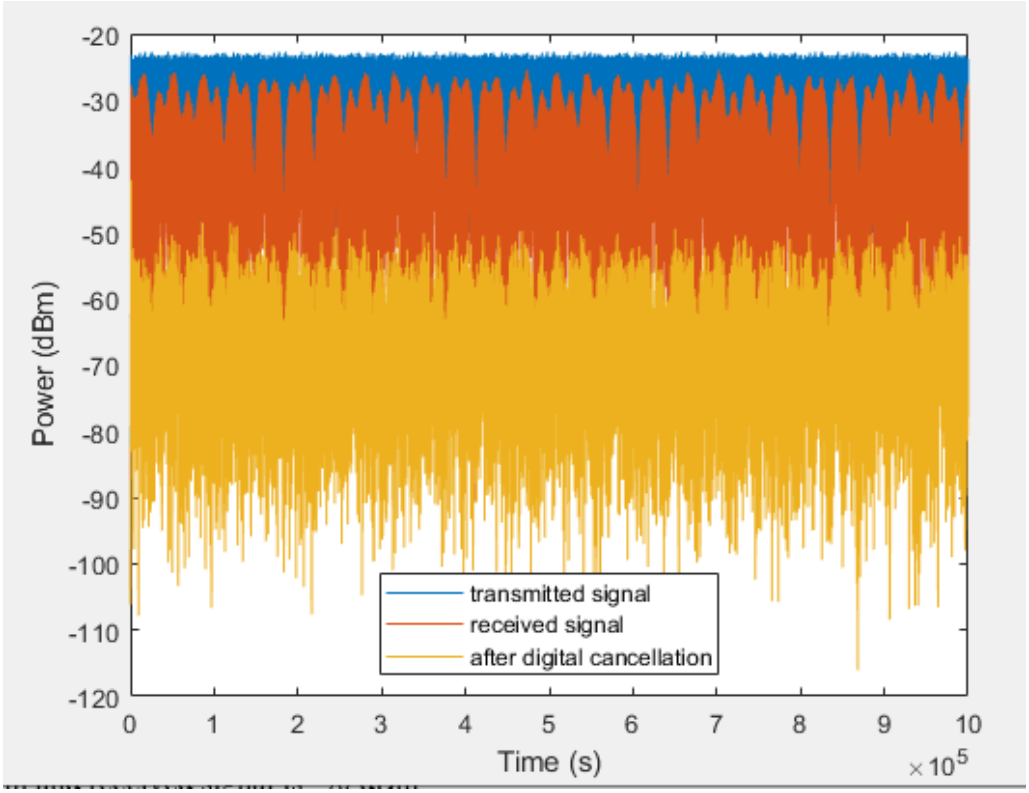

Figure 6.6. Plot of instantaneous signal power levels of the transmitted signal, received signal and signal after digital SI cancellation

Figure 6.6 shows the instantaneous power levels of the transmitted signal, received signal and signal after digital SI cancellation. The absolute power of the transmitted signal is -24.95 dBm and that of the received signal is -30.00 dBm. After digital SIC, the power of the received signal is -55.76 dBm. Therefore, the amount of achieved digital SI cancellation is 30.80 dB.

Case 2: Pseudo real-time implementation of FD system (with RF cables)

The flow graph for this case is explained in Section 5.4. The transmitter and receiver of the FD node are connected with the RF cable and also the remote transmitter and the receiver of the FD node are connected with the RF cable as well.

Table 6.4 lists the key parameters used for pseudo real-time implementation of the FD system with RF cables. The signal is transmitted through port TX1_1 from both Lime SDRs and received through port LNAH (RX1_H). Here, the transmitter path is denoted

by Power Amplifier (PA) path and the receiver path by Low Noise Amplifier (LNA) path.

Table 6.4. Key simulation parameters for real-time FD system (RF cable)

S.No	Block	Parameter	Value
1.	Constellation Modulator	Constellation	QPSK
		Sampling rate	1 MSPS
2.	Multiply Const	Constant	350 m
3.	Lime Suite Sink (TX)	Device Serial	0009070602461515
		RF Frequency	2.4 GHz
		Sample Rate	1 MSPS
		PA Path	Band 1
		Gain (dB)	52
4.	Lime Suite Source (RX)	Device Serial	0009070602461515
		RF Frequency	2.4 GHz
		Sample Rate	1 MSPS
		LNA Path	H
		Gain (dB)	37
5.	Lime Suite Sink (TX) (Remote transmitter)	Device Serial	0009070602461417
		RF Frequency	2.4 GHz
		Sample Rate	1 MSPS
		PA Path	Band 1
		Gain (dB)	35

In the GRC environment, it is very important to use exact device serial number to transmit and receive the signals with the boards. Here, the gain of the transmitters and receiver are adjusted empirically. The range of the transmitter gain of Lime SDR varies from 1 to 60 dB whereas the receiver gain can be adjusted from 1 to 70 dB. In real-time applications, generally the power of the received signal is -70 dBm. Therefore, to create this scenario, to make the power of the desired signal at the receiver approximately -70 dBm, the gain of the remote transmitter is adjusted at 35 dB. And the gain of the transmitter of FD node is adjusted to 52 dB because the SI signal is always stronger than the desired signal.

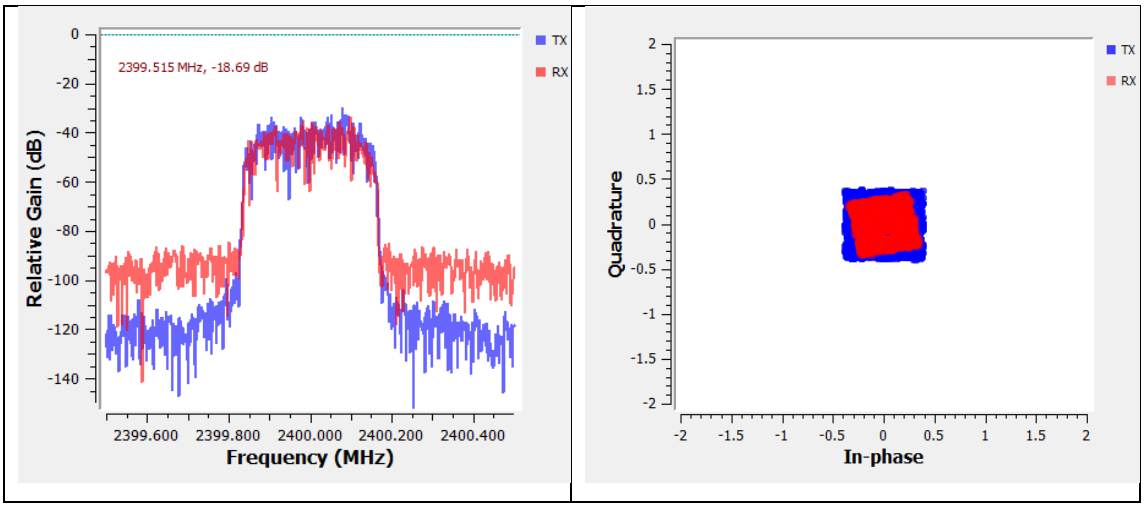

Figure 6.7. Frequency spectrum of transmitted and received signal (left) and constellation diagram of the transmitted symbols and received symbols (right), with RF cable

The frequency spectrum and constellation diagram of the transmitted and received (SI signal + desired signal) signals are presented in Figure 6.7. It can be observed from the left-hand side plot that the power levels of the transmitted signal and received signal are almost the same because the received signal consists of dominant SI signal as compared to the received desired signal. In addition, the constellation diagram of the received signal was observed to be stable and not scattered because the signal is received through RF cable without addition of significant noise and scattering of the signal. The intermediate results of timing recovery, equalizer, costas loop and constellation decoder are presented in Appendix 2. In the context of thesis, the main aim is to find the amount of digital SIC, which is discussed below.

Now, the digital SIC is performed using LMS algorithm in MATLAB by reading the files containing the transmitted signal and the received signal. The absolute power of the transmitted signal is -30 dBm and the received signal is -45.96 dBm. The amount of digital SIC depends on different factors such as length of training samples, step size and length of the estimation filter.

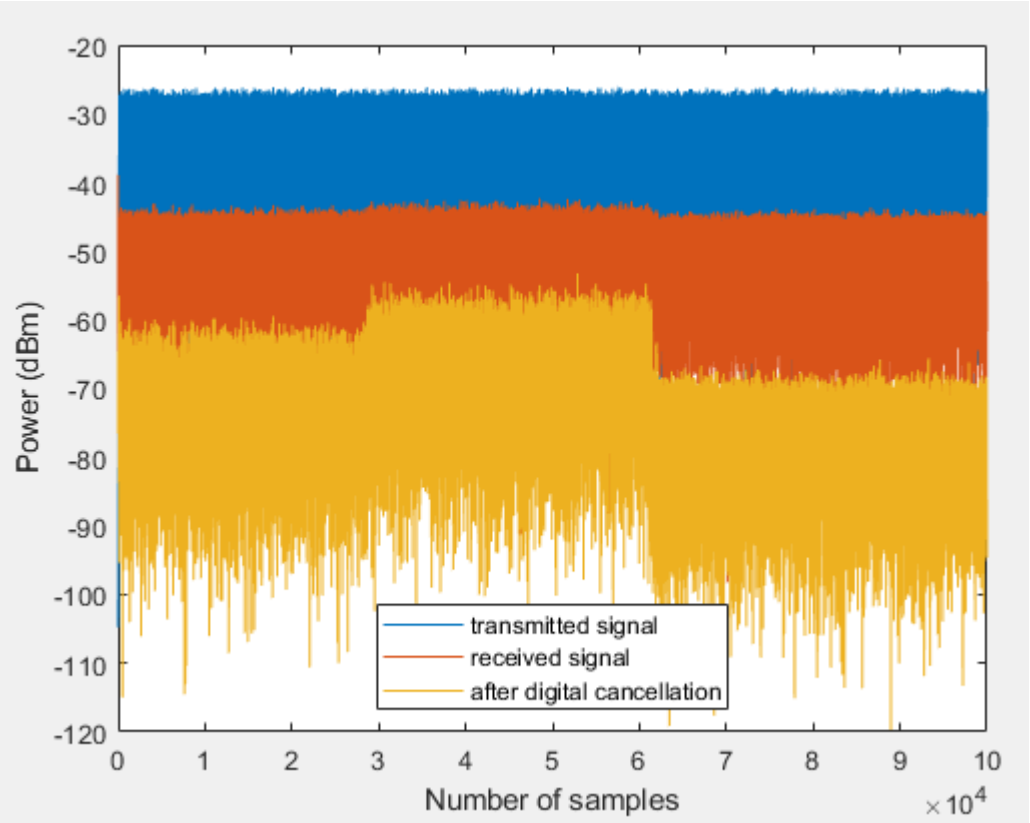

Figure 6.8. Plot of instantaneous signal power levels of the transmitted signal, received signal and signal after digital SI cancellation (RF cable)

The simulation parameters for the results of Figure 6.8 are step size (0.067), number of samples (500k) and length of the estimation filter taps (6). The absolute value of the signal after digital SIC is -65.75 dBm and the achieved amount of digital SIC is 19.79 dB. Now, let us see how different factors affects the amount of digital SIC.

- **Effect of length of the training samples**

In this experimental set up, the effect of length of the training samples on digital SIC amount has been studied with the step size of 0.067 and the length of the estimation filter taps is 6. The minimum value of the training samples is 1k while the maximum value is 900k. Figure 6.9 shows the effect of increasing the number of samples on amount of digital SIC.

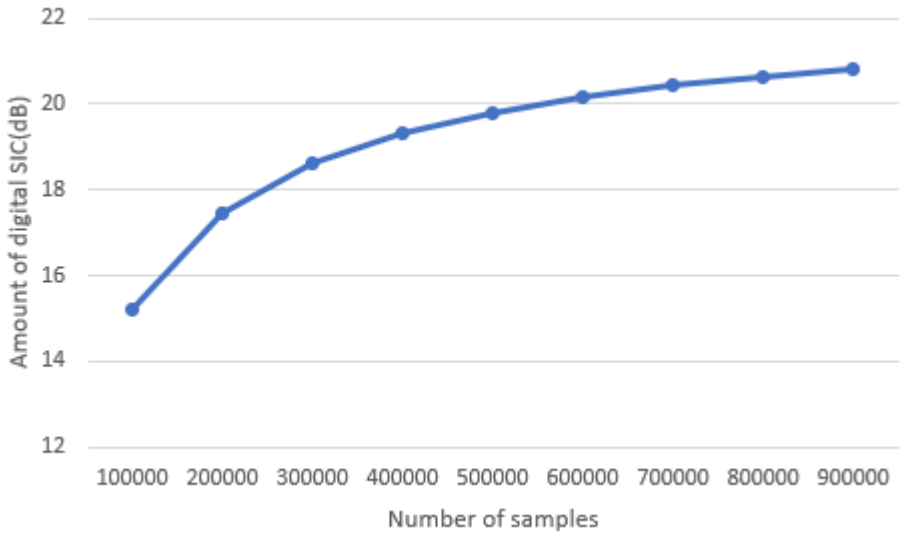

Figure 6.9. Amount of digital SIC vs the number of samples

It can be observed from Figure 6.9 that the amount of digital SIC increases with the number of samples. Although the processing time increases with the number of samples, in turn it provides a clear increase of the amount of digital SIC. For example, increasing the number of samples from 100k to 200k increases digital SIC by 3 dB approximately. It is also observed that the gains in the terms of SIC do not increase significantly after 500k samples.

- **Effect of Step Size**

In the next experimental set up, the effect of step size on the amount of SI cancellation has been studied with the different number of samples such as 100k, 500k and 900k; the length of the estimation filter is 6.

The amount of digital SIC is observed for five different step sizes of the LMS algorithm. In the Figure 6.10, the amount of digital SIC is calculated for different step sizes using different number of samples (100k, 500k and 900k). It can be seen from Figure 6.10 that the amount of digital SIC increases with the step size for a constant number of samples. The larger step size results in the faster convergence and increases the error (difference between the desired signal and the input signal of the LMS adaptive filter).

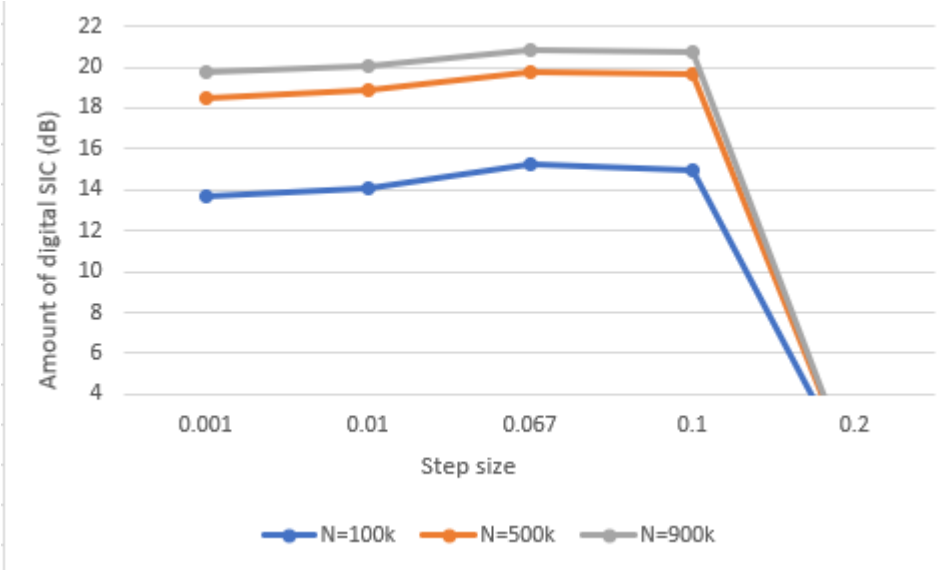

Figure 6.10. Effect of different step size on amount of digital SIC

As seen from Figure 6.10, for step size 0.1 and larger, the amount of digital SIC starts to decrease because of divergence of the error. This is because the step size should always satisfy the inequality given in Equation 3.7. Therefore, the larger step size increases the estimation error of the algorithm. The maximum amount of digital SIC has been observed for step size = 0.067, that is 15.22 dB for 100k samples, 19.79 dB for 500k samples, and 20.82 dB for 900k samples.

- **Effect of length of estimation filter**

In this experiment set up, the effect of the length of the adaptive filter (noted M) has been studied with 100k number of samples and step size (0.067). It can be observed from Figure 6.11 that; when there is a single tap (M=1) in the estimation filter yields the least amount of SIC (in the figure, lower values are better), whereas increasing the length of the estimation filter improves the SIC, up to a certain point (here for M=6). The output power of the digital canceller at M=1 is -51.81 dBm, for M=2; it is -60.18 dBm, and for M=6; it is -61.18 dBm. When M=7, the output power already increases to -61.09 dBm and for M=14, the observed power is -54.7 dBm. This means that some point increasing the filter length no longer increases the amount of digital SIC or decrease the output power of digital canceller.

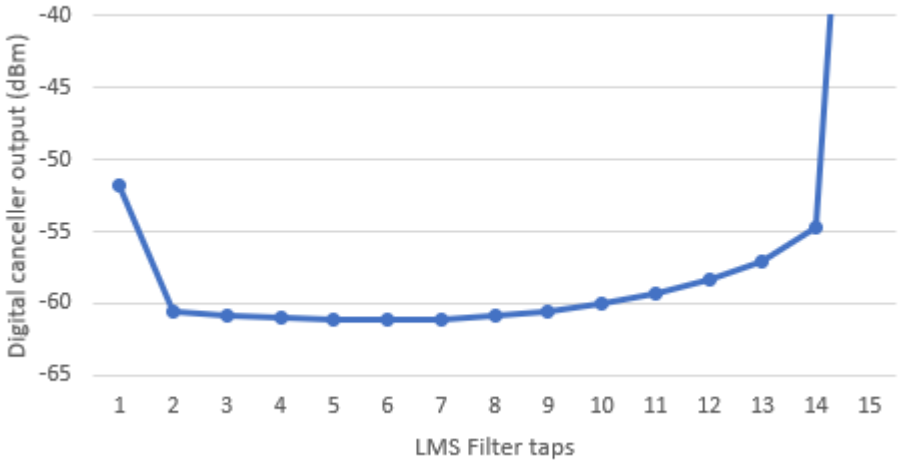

Figure 6.11. Absolute power of the digital canceller output for different length of estimation filter (smaller values are better)

Case 3: Pseudo real-time implementation of FD system (over the air)

The flow graph for this case is explained in Section 5.4. The transmission and reception of the signals take place over the air with antennas. All the parameters are same as presented in Table 6.4, except the gains of the transmitters and receiver. The gains of the transmitter and receiver of the FD node are 60 dB and 47 dB respectively, and the gain of the remote transmitter adjusted to 60 dB.

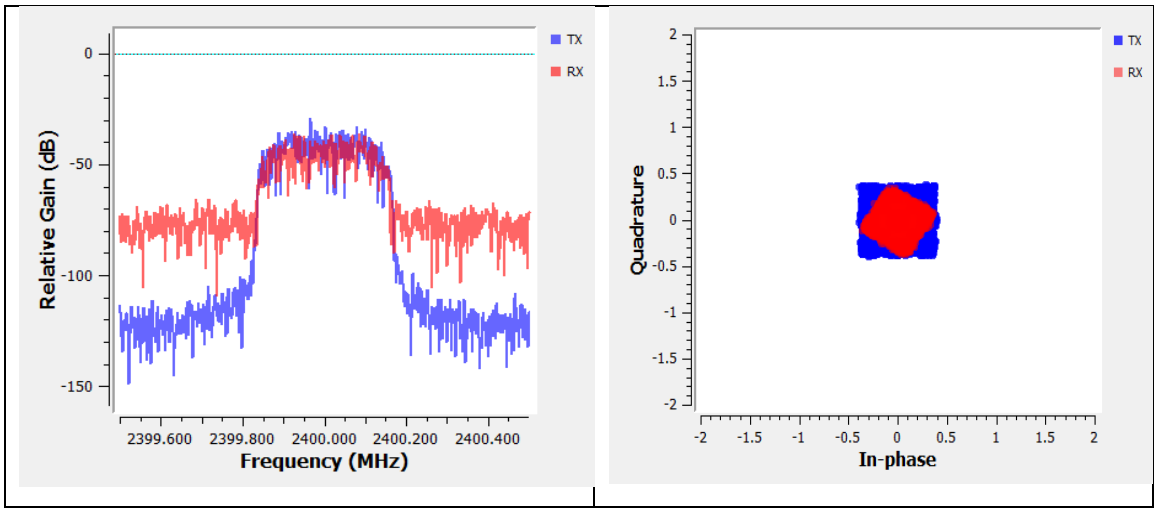

Figure 6.12. Frequency spectrum of transmitted and received signal (left) and constellation diagram of the transmitted symbols and received symbols (right), over the air

The frequency spectrum and constellation diagram of the transmitted and received (SI signal + desired signal) signal are presented in Figure 6.12. It can be seen from the left-hand plot that the received signal is shifted upwards as compared to the transmitted signal and the constellation is more scattered as compared to the transmission/reception through the RF cable, as expected. The constellation diagram of signals for over the air is more scattered with the same gain's values than that of the RF cable case; therefore, the gains of the transmitters and receiver are adjusted (transmitter gain = 60 dB, receiver gain=47 dB and remote transmitter gain = 60 dB) to improve the signal.

Now, the digital SIC is performed using LMS algorithm in MATLAB by reading the transmitted signal and the received signal. The absolute power of the transmitted signal is -39.12 dBm and the received signal is -42.86 dBm. Here, the absolute powers of the transmitted and received signals are different from the case with the RF cable because the gains of the transmitters and receiver are different for both cases. However, the point of interest is the amount of digital SIC.

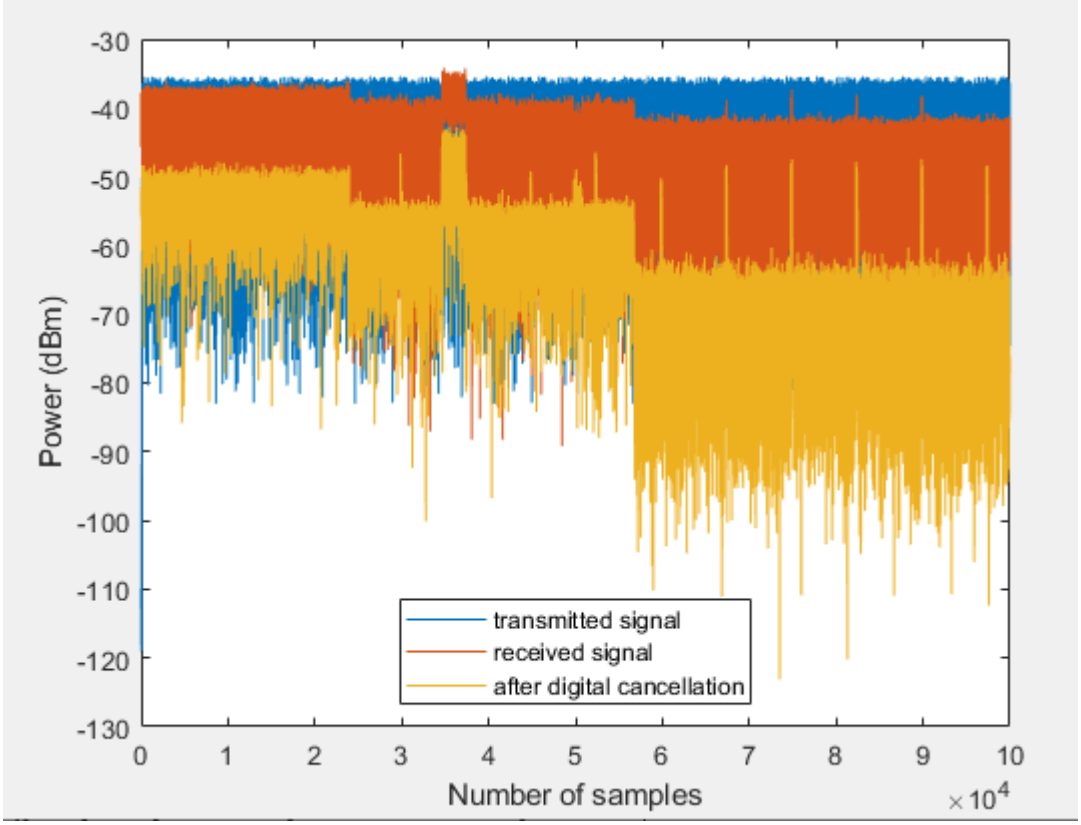

Figure 6.13. Plot of instantaneous signal power levels of the transmitted signal, received signal and signal after digital SI cancellation (over the air)

The parameters for the results shown in Figure 6.13 are step size (0.067), number of samples (500k) and length of the estimation filter taps (6). The absolute value of the signal after digital SIC is -50.54 dBm and the achieved amount of digital SIC is 7.48 dB.

Table 6.5 consists of the summarized results for the amount of digital SIC for different three cases for the same parameters, i.e. number of samples (500k), estimation filter length (6) and step size (0.067).

Table 6.5. Amount of digital SIC for different cases of implementation

Case	**Amount of digital SIC (dB)**
Simulation model	30.80
Pseudo real-time implementation with RF cable	19.79
Pseudo real-time implementation over the air	7.68

It can be seen from Table 6.5 that the maximum amount of digital SIC (30.80 dB) is achieved with simulation model but the value decreases for both real-time implementations. When the transmission/reception takes place through the RF cable, there is not significant addition of noise and scattering of the signal. Therefore, the achieved amount of digital SIC, although lower than in the simulation, is still significant with a value of 19.79 dB. In the case of over the air, the minimum amount of digital SIC is much lower (7.68 dB) because the received signal is noisier and more impacted by the multipath reflections. In [15], it is given that a real time digital canceller with low transmit power (0-10 dBm), i.e. same order of magnitude that can achieved with the Lime SDR-USB, can provide digital SI cancellation up to 25-35 dB. However, it is difficult to make a direct comparison because the experimentation is different, but this still gives an indication of what could be achieved. Some of the possible reasons for the limited performance of the implemented digital SIC are discussed in what follows.

In this thesis, the linear digital canceller is implemented using LMS algorithm. But the real-time signals comprise of non-linearities such as PA non-linearities, IQ imbalance and multipath reflections. These non-linearities can be eliminated by using a nonlinear digital SI canceller, and thus, the amount of digital SIC can be increased by using nonlinear digital cancellation technique. Moreover, self-interference cancellation is a

joint process of analog and digital cancellation. Therefore, if analog cancellation would be performed upstream of the digital cancellation then the nonlinear effects of PA and IQ imbalance can be minimized which in turn would help to increase the amount of SI cancellation.

6.3 Technical Challenges Faced During the Implementation and Solutions

It is well known that practical implementations are often challenging. This section comprises of some of the hurdles met during the implementation, and their solutions when applicable.

- The challenging part while implementing LMS, NLMS and RLS algorithms in MATLAB was to find the right parameters to achieve the desirable amount of digital SIC. Although, the range of the step size is calculated using an inequality expression, the precise value for maximum amount of digital SIC had to be found empirically.

- For the pseudo real-time implementation of FD system, the shape of the constellation diagram of the transmitted signal was initially not as expected. After extensive testing and troubleshooting, it appeared that the solution was very simple; i.e. to insert a Multiply Const block in between the Constellation Modulator and the Lime Suite Sink (TX). This solution was suggested by an external consultant and solved this issue at once.

- The digital SIC using LMS algorithm was not problematic as it had been implemented successfully for the performance analysis of the LMS, NLMS and RLS algorithms in the first part of this thesis. On the other hand, the offline mode consists of complex steps to read files in MATLAB from GRC environment, an additional steps based on cross correlation had to be implemented in order to align these read files before it is possible to perform the linear digital SIC using the LMS algorithm.

7 Conclusion

7.1 Summary

Full-duplex radios have the capability to create new possibilities to increase the spectral efficiency in situation where there are limited radio resources. A critical issue in implementing the FD radio is being able to mitigate the self-interference. Initially, full-duplex radios with different self-interference cancellation techniques have been studied and it was decided that this thesis should be mainly focussed on SIC in the digital domain.

The first aim of this thesis was to perform a comparative analysis of three adaptive algorithms, i.e. LMS, NLMS and RLS for digital SIC and their performance evaluation was based on simulations. The second main goal of this thesis was to design and implement a pseudo real-time digital SIC technique of FD system using SDR. Linear digital SIC was performed using LMS algorithm in offline mode. Moreover, the performance of the proposed system was evaluated for three scenarios, namely simulation model, transmission/reception with RF cable, and over the air.

Based on the simulation results, the performance of the RLS algorithm stands out from the simulated three algorithms. But, for real-time implementation, LMS algorithm is preferred over NLMS and RLS due to its computational simplicity, ease of implementation, unbiased convergence and lower implementation cost. Therefore, LMS algorithm was chosen for pseudo real-time implementation.

The simulation results obtained in this thesis show that a maximum amount of almost 31 dB of digital SIC can be achieved. Moreover, almost 20 dB and up to almost 8 dB digital SIC amounts are possible to achieve by using RF cable, and over the air respectively.

On the basis of these results, it can be concluded that the initial purpose of the thesis has been accomplished, i.e., the performance analysis of different algorithms (LMS, NLMS and RLS) for key figures of merits for digital SIC process for FD system has been conducted and a practical pseudo real-time realization thereof has been implemented and the influence of key factors on its performance has been analysed.

The results are encouraging and pave the way for further development of such digital self-interference cancellation process of full-duplex system, as briefly discussed in what follows.

7.2 Future Scope

In the context of this thesis, the future work can be divided into shorter-term perspective and longer-term perspectives.

- **Shorter-term perspectives**

It is possible to solve the multipath delay issue by adding multiple delay paths before injecting the transmitted signal to emulate an adaptive LMS filter. Moreover, a nonlinear digital self-interference could be implemented to cancel the nonlinear effects of the SI signal. Additionally, a nonlinear LMS algorithm could be used for the reconstruction of SI signal.

Furthermore, theoretically, the generalized sub-band decomposition LMS (GSD-LMS) algorithm shows improvements in convergence performance and reduces the computational complexity as compare to traditional LMS algorithm [34]. Its suitability and implementation to realize the digital SIC process could be investigated.

- **Longer-term perspectives**

Self-interference cancellation is a joint process of analog and digital cancellation. Therefore, if analog cancellation will be performed upstream of the digital cancellation then the nonlinear effects of PA and IQ imbalance can be minimized. A collaboration of these two-cancellation processes is expected to give better results. The implementation and evaluation of such a joint process is thus a natural longer-term perspective worth conducting.

References

[1] K. Parlin, T. Riihonen, R. Wichman, and D. Korpi, “Transferring the Full-Duplex Radio Technology from Wireless Networking to Defense and Security,” *Conf. Rec. - Asilomar Conf. Signals, Syst. Comput.*, vol. 2018-Octob, pp. 2196–2201, 2019.

[2] K. M. Thilina, H. Tabassum, E. Hossain, and D. I. Kim, “Medium access control design for full duplex wireless systems: Challenges and approaches,” *IEEE Commun. Mag.*, vol. 53, no. 5, pp. 112–120, 2015.

[3] S. K. Sharma, T. E. Bogale, L. B. Le, S. Chatzinotas, X. Wang, and B. Ottersten, “Dynamic Spectrum Sharing in 5G Wireless Networks with Full-Duplex Technology: Recent Advances and Research Challenges,” *IEEE Commun. Surv. Tutorials*, vol. 20, no. 1, pp. 674–707, 2018.

[4] D. Bharadia, E. McMilin, and S. Katti, “Full duplex radios,” *Comput. Commun. Rev.*, vol. 43, no. 4, pp. 375–386, 2013.

[5] E. Everett, A. Sahai, and A. Sabharwal, “Passive Self-Interference Suppression for Full-Duplex Infrastructure Nodes,” *IEEE Trans. Wirel. Commun.*, vol. 13, no. 2, pp. 1–16, 2013.

[6] C. E. Shannon, “A Mathematical Theory of Communication,” *Bell Syst. Tech. J.*, vol. 27, no. 3, pp. 379–423, 1948.

[7] E. Ahmed and A. M. Eltawil, “All-Digital Self-Interference Cancellation Technique for Full-Duplex Systems,” *IEEE Trans. Wirel. Commun.*, vol. 14, no. 7, pp. 3519–3532, 2015.

[8] S. Li and R. D. Murch, “An investigation into baseband techniques for single-channel full-duplex wireless communication systems,” *IEEE Trans. Wirel.*

Commun., vol. 13, no. 9, pp. 4794–4806, 2014.

[9] M. Chung, M. S. Sim, J. Kim, D. K. Kim, and C. B. Chae, "Prototyping real-time full duplex radios," *IEEE Commun. Mag.*, vol. 53, no. 9, pp. 56–63, 2015.

[10] A. Sahai, G. Patel, and A. Sabharwal, "Pushing the limits of Full-duplex: Design and Real-time Implementation," *arXiv:1107.0607*, 2011.

[11] Z. Zhang, X. Chai, K. Long, A. V. Vasilakos, and L. Hanzo, "Full duplex techniques for 5G networks: Self-interference cancellation, protocol design, and relay selection," *IEEE Commun. Mag.*, vol. 53, no. 5, pp. 128–137, 2015.

[12] M. S. Amjad and O. Gurbuz, "Linear digital cancellation with reduced computational complexity for full-duplex radios," *IEEE Wirel. Commun. Netw. Conf. WCNC*, no. 215, 2017.

[13] M. Zhou, N. Chen, C. Zhu, and Y. Yi, "Joint Digital Self-interference Cancellation in Full-duplex Radios under IQ Imbalance and Transmitter Non-linearity," *ITM Web Conf.*, vol. 17, p. 01003, 2018.

[14] J. Li, H. Zhang, and M. Fan, "Digital Self-Interference Cancellation Based on Independent Component Analysis for Co-Time Co-frequency Full-Duplex Communication Systems," *IEEE Access*, vol. 5, pp. 10222–10231, 2017.

[15] D. Korpi, M. Aghababaeetafreshi, M. Piilila, L. Anttila, and M. Valkama, "Advanced architectures for self-interference cancellation in full-duplex radios: Algorithms and measurements," *Conf. Rec. - Asilomar Conf. Signals, Syst. Comput.*, no. i, pp. 1553–1557, 2017.

[16] M. Aghababaeetafreshi, D. Korpi, M. Koskela, P. Jääskeläinen, M. Valkama, and J. Takala, "Software Defined Radio Implementation of a Digital Self-interference Cancellation Method for Inband Full-Duplex Radio Using Mobile Processors," *J. Signal Process. Syst.*, vol. 90, no. 10, pp. 1297–1309, 2018.

[17] M. Yilan, O. Gurbuz, and H. Ozkan, "Nonlinear digital self-interference cancellation for full duplex communication," *Phys. Commun.*, vol. 35, p. 100698, 2019.

[18] E. A. Gharavol and E. G. Larsson, Robust joint optimization of MIMO two-way relay channels with imperfect CSI, *49th Annual Allerton Conference on Communication, Control, and Computing (Allerton)*vol. 2, no. 12. 2011.

[19] M. Jain *et al.*, "Practical, real-time, full duplex wireless," *Proc. Annu. Int. Conf. Mob. Comput. Networking, MOBICOM*, pp. 301–312, 2011.

[20] K. Kumud, "Adaptive Self-Interference Cancellation in Full-Duplex Radio,"M.S.Thesis, Faculty of Computing and Electrical Engineering, Tampere University of Technology, 2015. Accessed on: October 13, 2019.[online]. Available: https://pdfs.semanticscholar.org/ccee/8caa 6f21cf768dc633ebacef1c21 ae2cb478.pdf

[21] M. Duarte, C. Dick, and A. Sabharwal, "Experiment-driven characterization of full-duplex wireless systems," *IEEE Trans. Wirel. Commun.*, vol. 11, no. 12, pp. 4296–4307, 2012.

[22] S. P. Yadav and S. C. Bera, "Nonlinearity effect of high power amplifiers in communication systems," *Proc. - 2014 IEEE Int. Conf. Adv. Commun. Comput. Technol. ICACACT 2014*, pp. 1–6, 2015.

[23] L. Anttila, D. Korpi, V. Syrjälä, and M. Valkama, "Cancellation of power amplifier induced nonlinear self-interference in full-duplex transceivers," *Conf. Rec. - Asilomar Conf. Signals, Syst. Comput.*, pp. 1193–1198, 2013.

[24] M. Makurzdi, V. Valimaki, and J. T. I. Lankso, "Closed-form design of tunable fractional-delay allpass filter structures," *IEEE Int. Sym. on Circuits and Syst*, pp. 434–437,2001.

[25] S.Haykin, *Adaptive Filter Theory*, 3rd ed. Prentice-Hall, 2007.

[26] N. S. Adapa and S. Bollu, "Performance Analysis of different Adaptive Algorithms based on Acoustic Echo Cancellation," M.S.Thesis, Department of Engineering, Blekinge Institute of Technology, Sweden, 2012.Accessed on: March 13, 2020.[online] Available: https://pdfs.semanticscholar.org/ ec6e/ 5d18762c6fb3d91b703dbc8ce368ffaf4038.pdf

[27] Mathworks.com, “No Title,” *Compare-rls-and-lms-adaptive-filter-algorithms*, 2019. [Online]. Available: https://se.mathworks.com/help/dsp/ug/compare-rls-and-lms-adaptive-filter-algorithms.html. [Accessed: 22-Feb-2020].

[28] T. S. Rappaport, “Wireless Communications, Principles and Practice", *Prentice Hall, 2nd edition, ISBN 0130422320.pdf*. 2002.

[29] S. Saunders and A. Aragón, *Antennas and Propagation for Wireless Communication Systems, 2nd ed, John Wiley & Sons, Chichester*. 2007.

[30] N. Kostov, “Mobile radio channels modeling in MATLAB,” *Radioengineering*, vol. 12, no. 4, pp. 12–16, 2003.

[31] “No Title.” [Online]. Available: https://wiki.myriadrf.org/LimeSDR-USB. [Accessed: 23-Apr-2020].

[32] F.J.Harris and M.Rice, *Multirate Digital Filters for Symbol Timing Synchronization in Software Defined Radios*, Vol. 19, N. IEEE Selected Areas in Communications, 2001.

[33] Y. Amarbabu, “Design and Implementation of Adaptive Filters for Real Time Applications,” *IJARECE*, vol. 4, no. 5, pp. 1112–1116, 2015.

[34] Z. Chen and G. Yue, “LMS Algorithm Based on Subband Decomposition,” *Int. Conf. Commun. Technol. Proceedings, ICCT*, vol. 1, 1998.

Appendix 1 – Linear Digital SIC of FD System

Source code for performance analysis of LMS, NLMS and RLS algorithms.

```
clear all
close all
j=1i;
%% Parameters
N = 1e3; % Total TX symbol number
Trial = 1e3; % Trial number

% Channel Norm error
Psi_a_norm_error_average_LMS = zeros(N,1);
Psi_a_norm_error_average_NLMS = zeros(N,1);
Psi_a_norm_error_average_RLS = zeros(N,1);
% error
Desired_y_error_average_LMS = zeros(N,1);
Desired_y_error_average_NLMS = zeros(N,1);
Desired_y_error_average_RLS = zeros(N,1);
% SIR (Signal to residual interference ratio)
SIR_average_LMS = zeros(N,1);
SIR_average_NLMS = zeros(N,1);
SIR_average_RLS = zeros(N,1);
%% Trial Loop
for t = 1:Trial
    %% Signal
    M = 4; % QPSK signal
    s_pre = pskmod(randi([0 M-1],N,1),M,pi/4); % Un-Known signal
    x_pre = pskmod(randi([0 M-1],N,1),M,pi/4); % Known signal

    s = ifft(s_pre)*sqrt(N);
    x = ifft(x_pre)*sqrt(N);

    %% Channel
    Channel_length = 5;
    H = (randn(Channel_length,2)*[1;j]/sqrt(2)); % Rayleigh channel
[5x1]

    SIR_pre = -20; % dB %% SIR
    Psi =  10.^(-SIR_pre/10/2)*[0.19+.56j .45-1.28j -.14-.53j -
.19+.23j .33+.51j]; % fd=80Hz and k =3

    %% AWGN Noise
    SNR = 20;
    np = 10.^(-SNR/20); % noise power, Eb = 1 dB
    n = sqrt(np)*randn(N,2)*[1;j]/sqrt(2);
    %%  Initial Parameters
    Desired = zeros(N,1);
    Self_Interference = zeros(N,1);

    % Channel Norm error
    Phi_a_norm_error_LMS = zeros(N,1);
    Phi_a_norm_error_NLMS = zeros(N,1);
    Phi_a_norm_error_RLS = zeros(N,1);
```

```
    % SIR
    SIR_LMS = zeros(N,1);
    SIR_NLMS = zeros(N,1);
    SIR_RLS = zeros(N,1);

      % Cancellation process
    a_length = 5;
    a_LMS = zeros(a_length,1);  % Initial weigth
    a_NLMS = zeros(a_length,1);
    a_RLS = zeros(a_length,1);  % Initial weigth
    y_LMS = zeros(N,1);
    y_NLMS = zeros(N,1);
    y_RLS = zeros(N,1);

     % RLS Initial
    epsilon = 0.0001;
    P = (epsilon^-1)*eye(a_length);
    %% Main program
    for index = a_length:N
        Desired(index) = H'*s(index:-1:index-(Channel_length-1));
        Self_Interference(index) = Psi'*x(index:-1:index-
(Channel_length-1));

        % LMS
        y_LMS(index) = Desired(index) + Self_Interference(index) -
a_LMS'*x(index:-1:index-(a_length-1)) + n(index);
        a_LMS = DF_LMS_function(a_LMS,y_LMS(index),x(index:-1:index-
(a_length-1)));
        Phi_a_norm_error_LMS(index) = 10*log10(norm(Psi-
a_LMS(1:Channel_length))^2); % dB

        % NLMS
        y_NLMS(index) = Desired(index) + Self_Interference(index) -
a_NLMS'*x(index:-1:index-(a_length-1)) + n(index);
        a_NLMS = DF_NLMS_function(a_NLMS,y_NLMS(index),x(index:-
1:index-(a_length-1)));
        Phi_a_norm_error_NLMS(index) = 10*log10(norm(Psi-
a_NLMS(1:Channel_length))^2); % dB

        % RLS
        y_RLS(index) = Desired(index) + Self_Interference(index) -
a_RLS'*x(index:-1:index-(a_length-1)) + n(index);
        [a_RLS,P] = DF_RLS_function(a_RLS,y_RLS(index),x(index:-
1:index-(a_length-1)),P);
        Phi_a_norm_error_RLS(index) = 10*log10(norm(Psi
a_RLS(1:Channel_length))^2); % dB
    end
    Psi_a_norm_error_average_LMS = Psi_a_norm_error_average_LMS +
Phi_a_norm_error_LMS/Trial; % dB
    Psi_a_norm_error_average_NLMS = Psi_a_norm_error_average_NLMS +
Phi_a_norm_error_NLMS/Trial; % d
    Psi_a_norm_error_average_RLS = Psi_a_norm_error_average_RLS +
Phi_a_norm_error_RLS/Trial; % dB

    Desired_y_error_average_LMS = Desired_y_error_average_LMS +
20*log10(abs(y_LMS - Desired))/Trial; % dB
    Desired_y_error_average_NLMS = Desired_y_error_average_NLMS +
20*log10(abs(y_NLMS - Desired))/Trial; % dB
```

```
    Desired_y_error_average_RLS = Desired_y_error_average_RLS +
20*log10(abs(y_RLS - Desired))/Trial; % dB

    SIR_average_LMS = SIR_average_LMS +
20*log10(abs(Desired)./abs(Desired-y_LMS)) /Trial; % dB
    SIR_average_NLMS = SIR_average_NLMS +
20*log10(abs(Desired)./abs(Desired-y_NLMS)) /Trial; % dB
    SIR_average_RLS = SIR_average_RLS +
20*log10(abs(Desired)./abs(Desired-y_RLS)) /Trial; % dB
end % Trial Loop
% % Plot
%-------------------------------------------------------------%
figure(1),stem(abs(Psi),'o','Linewidth',2);
hold on;
figure(7),stem(abs(a_LMS(1:Channel_length)),'--x','Linewidth',2);
figure(7),stem(abs(a_NLMS(1:Channel_length)),':^','Linewidth',2);
figure(7),stem(abs(a_RLS(1:Channel_length)),':^','Linewidth',2);
hold off
title('Self Channel Estimation');
xlabel('Order');ylabel('');
axis square;
legend('|\Psi|^2','|a_L_M_S|^2','|a_N_L_M_S|^2','|a_R_L_S|^2');

figure(2),plot(Desired_y_error_average_LMS);
hold on
figure(8),plot(Desired_y_error_average_NLMS);
hold on
figure(8),plot(Desired_y_error_average_RLS);
hold off
title('|d_n - y_n|^2');xlabel('Iteration
(Symbol)');ylabel('dB');legend('LMS','NLMS ','RLS');

figure(3),plot([1,N],[SNR,SNR],':','Color',[0.4660 0.6740
0.1880],'Linewidth',2);
hold on
figure(9),plot(SIR_average_LMS,'Color',[0 0.4470 0.7410]);
figure(9),plot(SIR_average_NLMS,'Color',[0.8500 0.3250 0.0980]);
figure(9),plot(SIR_average_RLS,'Color',[0.9290 0.6940 0.1250]);
hold off
title('SINR');xlabel('Iteration (Symbol)');ylabel('dB');legend('Self-
Interference free floor','LMS','NLMS','RLS');
```

Appendix 2 – Pseudo Real-Time Implementation of FD System (with RF cable)

1. Intermediate results to understand the receiver design

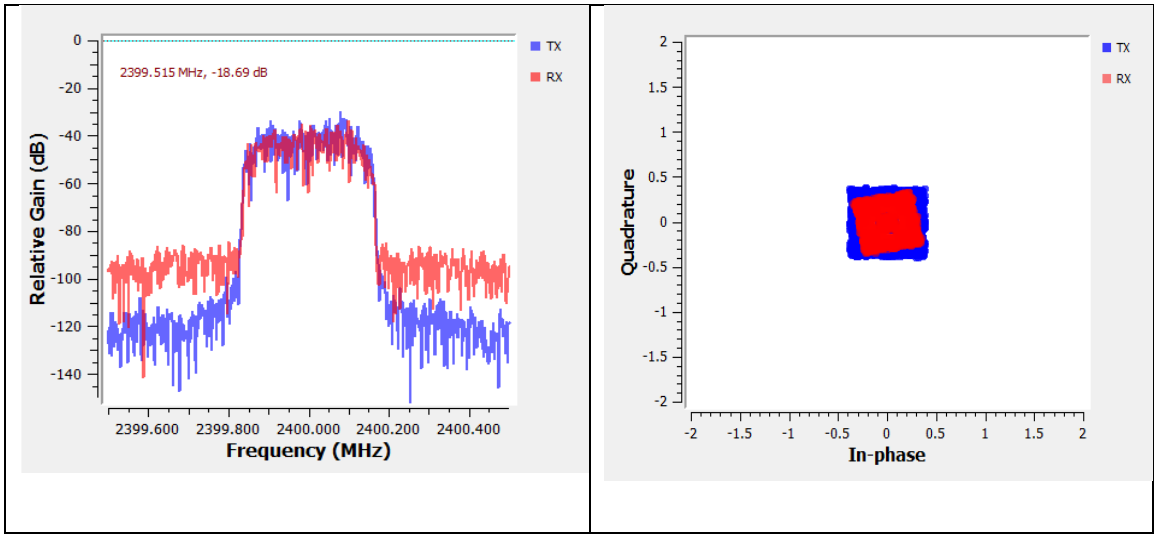

Figure A2.1. Frequency spectrum and constellation diagram of transmitted and received signal

Stage 1: Polyphase Clock Synchronizer – Timing recovery

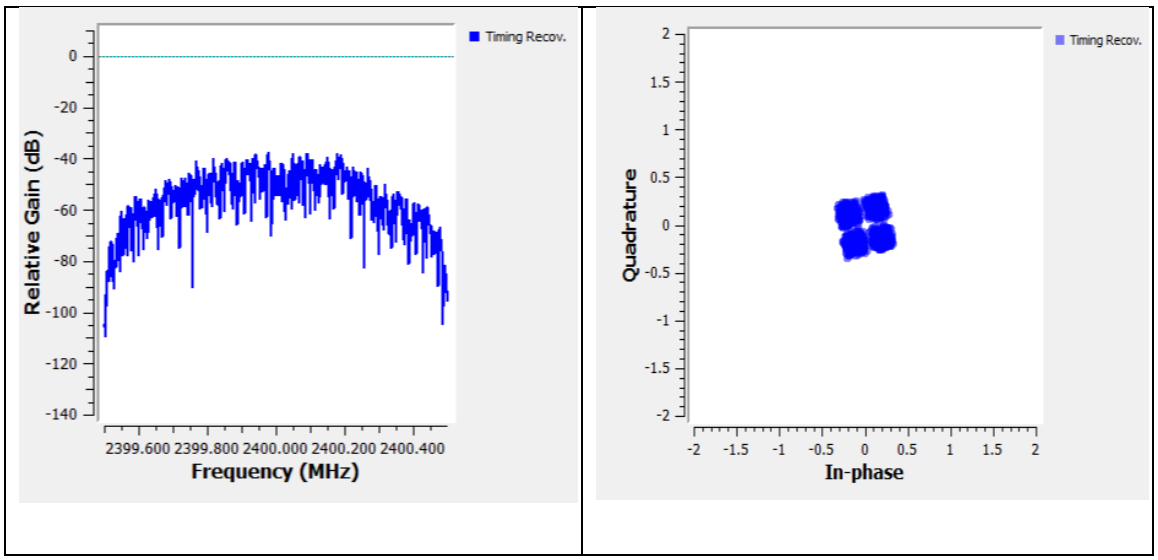

Figure A2.2. Frequency spectrum and constellation diagram after timing recovery

Stage 2: CMA Equalizer

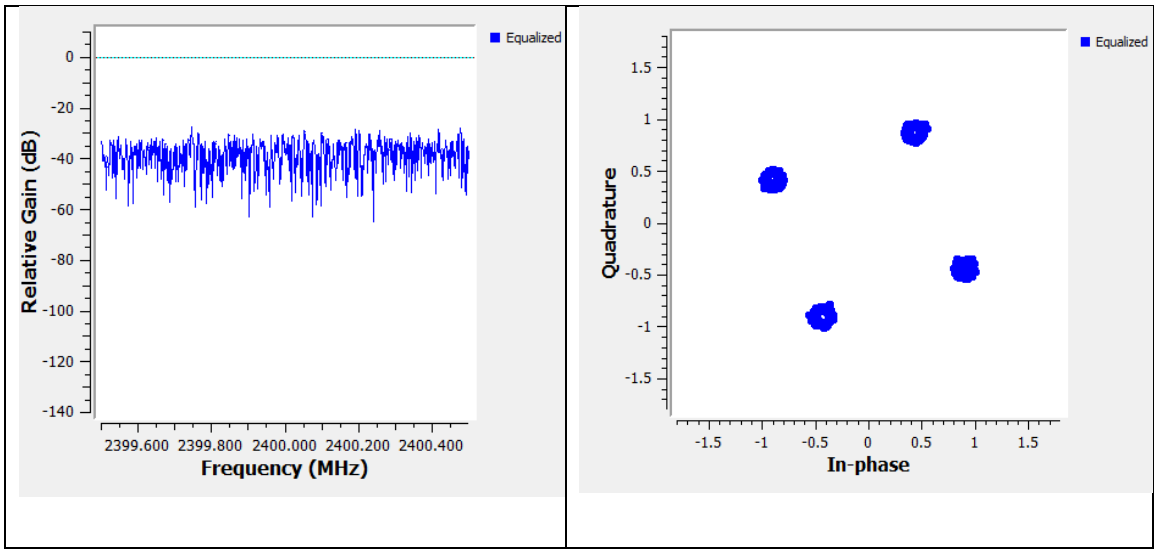

Figure A2.3. Frequency spectrum and constellation diagram after equalization

Stage 3: Costas Loop and Constellation decoder

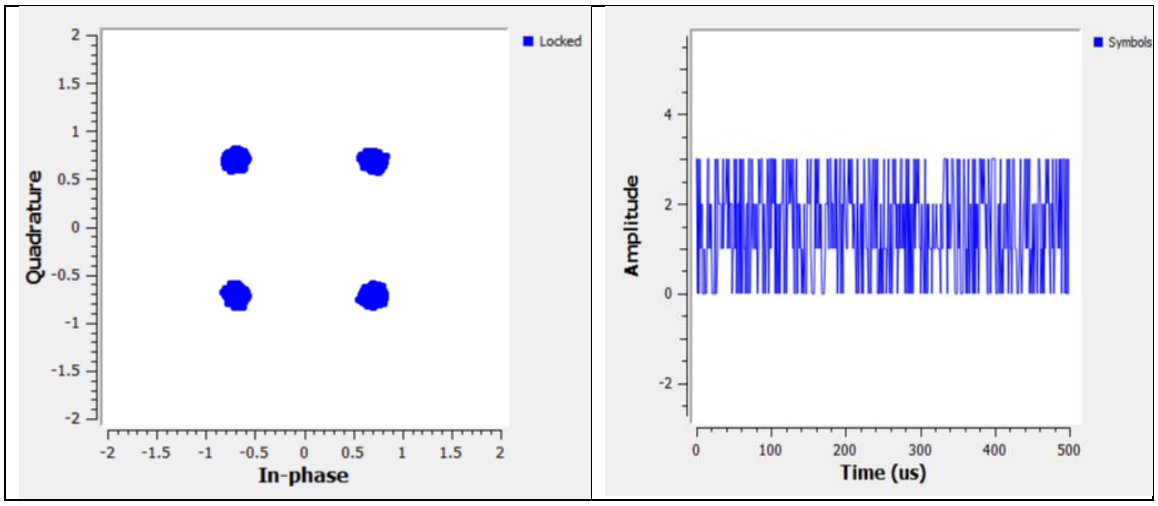

Figure A2.4. Locked constellation diagram (left) and decoded symbols (right)

2. Source code of digital SIC using LMS algorithm in offline mode

```
Nmax = 100e3;
Fs = 100e3; %% sampling frequency
N = 400e3; %% number of samples

name = input('Enter the name of a file: ','s');
x=importdata(name);%% transmitted signal
name_1 = input('Enter the name of a file: ','s');
```

```
y2=importdata(name_1);%% received signal

a_length = 6; %% estimation channel length
a_LMS = zeros(a_length,1);  % Initial weigth

 for index = a_length:N
 y3(index) = y2(index)-a_LMS'*x(index:-1:index-(a_length-1));
 a_LMS = DF_LMS_function(a_LMS,y3(index),x(index:-1:index-(a_length-
1)));
 end

% %% calculate and display power levels
P = var(x);
P1_dBm = 10*log10(P/1*10^-3);
P2_dB = var(y2);
P2_dBm = 10*log10(P2_dB/1*10^-3);
P3_dB = var(y3);
P3_dBm = 10*log10(P3_dB/1*10^-3);

disp(['    transmitted signal: '  num2str(P1_dBm) ' dBm']);
disp(['     received signal: '  num2str(P2_dBm) ' dBm']);
disp(['    after digital cancellation: '  num2str(P3_dBm) ' dBm']);
disp(['amount of digital cancellation:  ' num2str(P2_dBm-P3_dBm) '
dB']);

% %% plot instantaneous signal power
figure(4); clf;
plot(1e5*(0:Nmax-1)/Fs, -30+10*log10(abs(x(1:Nmax).^2))); hold on;
plot(1e5*(0:Nmax-1)/Fs, -32+10*log10(abs(y2(1:Nmax).^2)));
plot(1e5*(0:Nmax-1)/Fs, -34+10*log10(abs(y3(1:Nmax).^2)));

xlabel('Number of samples')
ylabel('Power (dBm)')
legend('transmitted signal', 'received signal', 'after digital
cancellation', 'location','south');
```